THE ROLE OF PROTEIN-MEMBRANE INTERACTIONS IN MODULATION OF SIGNALING BY BACTERIAL CHEMORECEPTORS

A Dissertation

by

ROGER RUSSELL DRAHEIM

Submitted to the Office of Graduate Studies of
Texas A&M University
in partial fulfillment of the requirements for the degree of

DOCTOR OF PHILOSOPHY

May 2007

Major Subject: Microbiology

THE ROLE OF PROTEIN-MEMBRANE INTERACTIONS IN MODULATION OF SIGNALING BY BACTERIAL CHEMORECEPTORS

A Dissertation

by

ROGER RUSSELL DRAHEIM

Submitted to the Office of Graduate Studies of
Texas A&M University
in partial fulfillment of the requirements for the degree of

DOCTOR OF PHILOSOPHY

Approved by:

Chair of Committee,	Michael D. Manson
Committee Members,	Deborah Bell-Pedersen
	David P. Giedroc
	Deborah A. Siegele
Head of Department,	Vincent M. Cassone

May 2007

Major Subject: Microbiology

ABSTRACT

The Role of Protein-Membrane Interactions in Modulation of Signaling by Bacterial Chemoreceptors. (May 2007)

Roger Russell Draheim,

B.S.; B.S., University of Maine

Chair of Advisory Committee: Dr. Michael D. Manson

Environmental signals are sensed by membrane-spanning receptors that communicate with the cell interior. Bacterial chemoreceptors modulate the activity of the CheA kinase in response to binding of small ligands or upon interaction with substrate-bound periplasmic-binding proteins. The mechanism of signal transduction across the membrane is a displacement of the second transmembrane domain (TM2) a few angstroms toward the cytoplasm. This movement repositions a dynamic transmembrane helix relative to the plane of the cell membrane. The research presented in this dissertation investigated the contribution of TM2-membrane interactions to signaling by the aspartate chemoreceptor (Tar) of *Escherichia coli*. Aromatic residues that reside at the cytoplasmic polar-hydrophobic membrane interface (Trp-209 and Tyr-210) were found to play a significant role in regulating signaling by Tar. These interactions were subsequently manipulated to modulate the signaling properties of Tar. The baseline signaling state was shown to be incrementally altered by repositioning the Trp-209/Tyr-210 pair. To our knowledge, this is the first example of harnessing membrane-protein interactions to modulate the signal output of a transmembrane receptor in a controlled and predictable manner. Potential long-term applications include

the use of analogous mutations to elucidate two-component signaling pathways, to engineer the signaling parameters of biosensors that incorporate chemoreceptors, and to predict the movement of dynamic transmembrane helices *in silico*.

I dedicate this dissertation to my wife and best friend, Heather Lynn Draheim, for her unwavering support during my graduate studies.

ACKNOWLEDGEMENTS

I am grateful to have had the privilege to work with very talented colleagues. Throughout the years, my “Mike Manson Friends” provided the perfect blend of camaraderie, encouragement, support, knowledge and criticism. Within this group, additional recognition should be given to Drs. Brian J. Cantwell and Run-Zhi Lai, with whom many ideas were shared, critiqued, and seen through to fruition. I can only hope that I have reciprocated their contributions and that future group members will find this dissertation both useful and insightful.

I, also, appreciate the members of my doctoral advisory committee for overseeing my development as a graduate student. I am deeply indebted to the chair of my committee, Dr. Michael D. Manson, who had the gargantuan task of molding a naive graduate student into a young investigator. I can only imagine how difficult this task was and I greatly appreciate his perseverance.

I would, also, like to acknowledge my family for their insistence on attaining a higher education. Above all, I wish to acknowledge my wife, Heather Lynn Draheim, because without her continued support I would not be the person I am today.

TABLE OF CONTENTS

LIST OF FIGURES

FIGURE Page

LIST OF TABLES

CHAPTER I

INTRODUCTION

E. coli responds to a variety of environmental stimuli

Escherichia coli is a rod-shaped, nonsporulating, Gram-negative bacterium. Individual cells are small, measuring approximately 1-2 μm in length and 0.1-0.5 μm in diameter, and as individual cells they cannot change their surroundings to a significant extent. Therefore, to remain viable, planktonic bacteria must respond to changing environmental conditions. Chemotaxis is one mechanism bacterial use to adapt to such changes (*1*). *E. coli* responds to a wide variety of chemical signals, including pH (*2*), redox potential (*3, 4*), and concentration gradients of amino acids (*5*), sugars (*6*), small peptides (*7*), and certain noxious organic compounds and divalent cations (*2*).

E. coli cells possess five to seven flagella distributed over their cellular surface (*8*). Each flagellum is driven by an independent bidirectional rotary motor (*9*). Counterclockwise (CCW) rotation of these motors allows the flagellar filaments, which are lefthanded helices, to coalesce into a bundle at one end of the cell and propel it in a relatively linear run (*10*). CW rotation of at least one flagellum disrupts this bundle, resulting in an active reorientation in three-dimensional space known as a tumble (*11*) (Figure 1.1A). The greater the number of flagella that rotate CW, the more rapid and complete the reorientation.

This dissertation follows the style of *Biochemistry*.

In a homogeneous environment, *E. coli* performs a three-dimensional random walk in which smooth swims (runs) lasting several seconds alternate with tumbles (Figure 1.1B). As they swim, cells are constantly comparing their environment to one they experienced a few seconds earlier (*12-14*). This temporal comparison gives cells the information they need to increase the length of runs that happen to lead in a favorable direction, whether up an attractant gradient or down a repellent gradient. This selective biasing of the random walk generates net migration in gradients of chemoeffectors (Figure 1.1C).

A phosphorelay couples detection of stimuli to changes in cellular behavior

A series of protein phosphorylations (phosphorelay) couples the detection of chemoeffectors to changes in the direction of flagellar rotation (Figure 1.2). Within *E. coli*, each of the four members of a family of homodimeric chemoreceptors detects a specific set of chemoeffectors. The receptors normally activate the histidine protein kinase CheA (*15*), which is coupled to the receptors via the adaptor protein CheW. Interaction of CheA dimers with the chemoreceptors causes a hundred-fold increase in the rate of autophosphorylation of a specific histidyl residue (*16*) within each monomer (*15*). The phosphoryl group is then transferred to an aspartyl residue within the response regulator CheY (*16*). Phospho-CheY binds to FliM in the flagellar motor to promote clockwise (CW) rotation of the flagella (*17, 18*). The relative activities of CheA and the CheY-P phosphatase CheZ establish the ratio of CheY to CheY-P within the cell, and hence control the frequency of tumbling (*15, 19*) (Figure 1.2A).

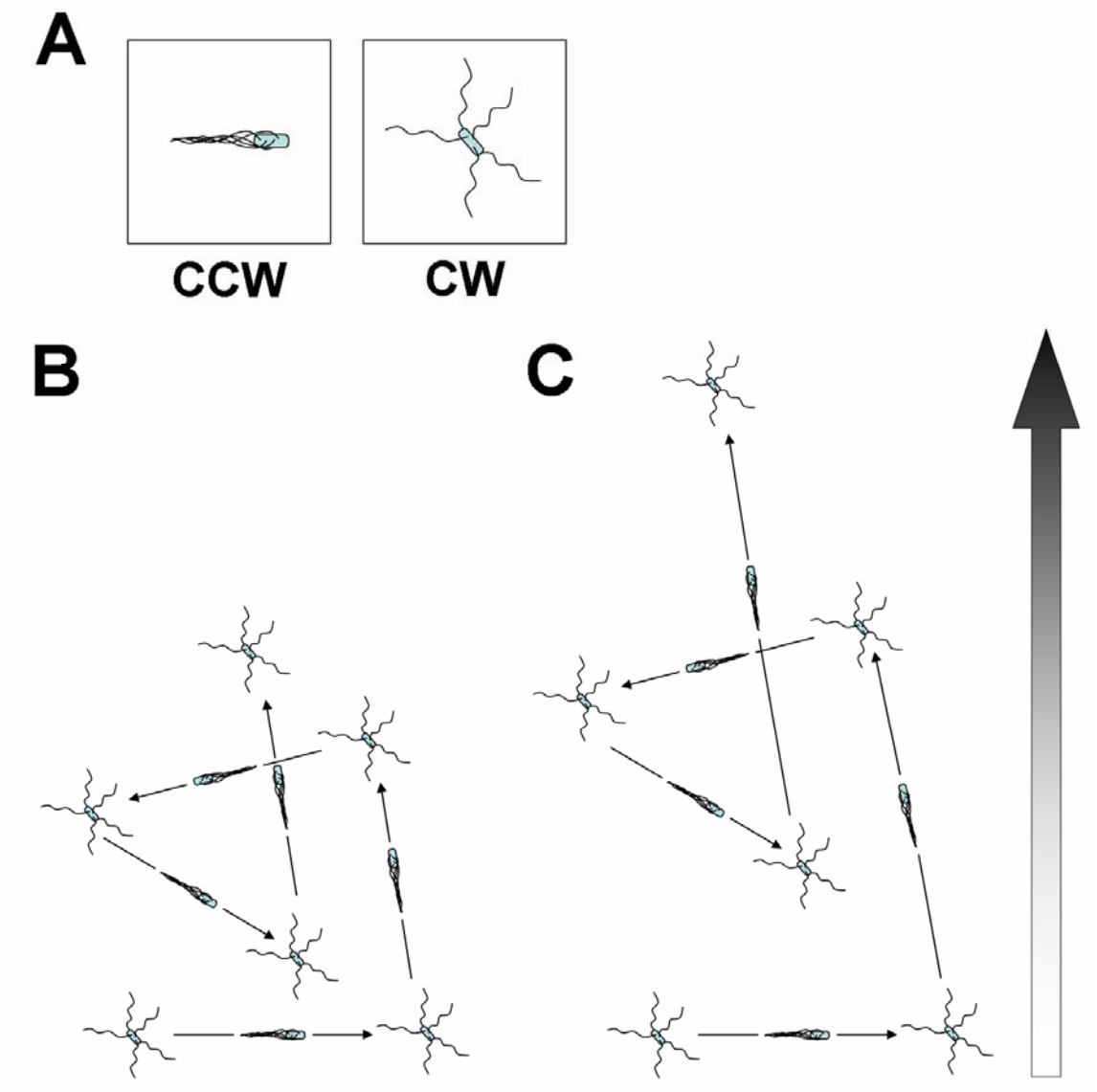

Figure 1.1 Chemotaxis of *E. coli* in a gradient of chemoeffector. (A) Counterclockwise (CCW) rotation allows the flagella to coalesce at one end of cell and propel it in a relatively linear fashion. Clockwise (CW) rotation of one or more flagella results in a tumbling event that randomly reorients that cell in three-dimensional space. (B) In a homogeneous environment, cells perform a random walk composed of alternating runs and tumbles. (C) In the presence of an attractant, the probability of a tumbling event (CW) decreases during running events that lead in a favorable direction. This biases the random walk (B) to allow net migration toward higher concentrations of attractant (shaded portion of the arrow) or lower concentrations of repellent.

The conformational changes induced by an attractant stimulus convert a chemoreceptor from a hundred-fold stimulator of CheA activity into a five-fold inhibitor (*20*) (Figure 1.2B). The resulting drop in phospho-CheY, which is accelerated by CheZ, suppresses tumbling and lengthens runs toward higher concentrations of attractant. Repellents increase the intracellular level of phospho-CheY, thereby lengthening runs that lead away from higher concentrations of repellents. Changes in CheA activity are balanced by covalent methylation of the cognate receptor (*21*) (Figure 1.2C). Methyl groups are added by a methyltransferase, CheR, and removed by CheB, a methylesterase (*22, 23*). CheB is active when it is phosphorylated by CheA (*24*). Increased methylation of four specific glutamyl residues in the cytoplasmic domain of the chemoreceptor biases it toward CheA stimulation, whereas decreased methylation results in less CheA stimulation (*25, 26*).

The antagonistic effects of attractant binding and covalent methylation are essential for chemotactic behavior. When cells are moving in gradients of chemoeffectors, constant adjustment of the extent of receptor methylation allows for a temporal comparison of the current environment to one from few seconds ago. In this manner, methylation serves as a rudimentary chemical "memory" (*12, 13*). In addition, at various constant concentrations of extracellular chemoeffector, the interplay between ligand occupancy and receptor methylation allows cells to maintain the same baseline level of CheA activity (*27*). Maintaining this optimal run/tumble bias provides enhanced sensitivity to chemoeffectors over a wide range of concentrations.

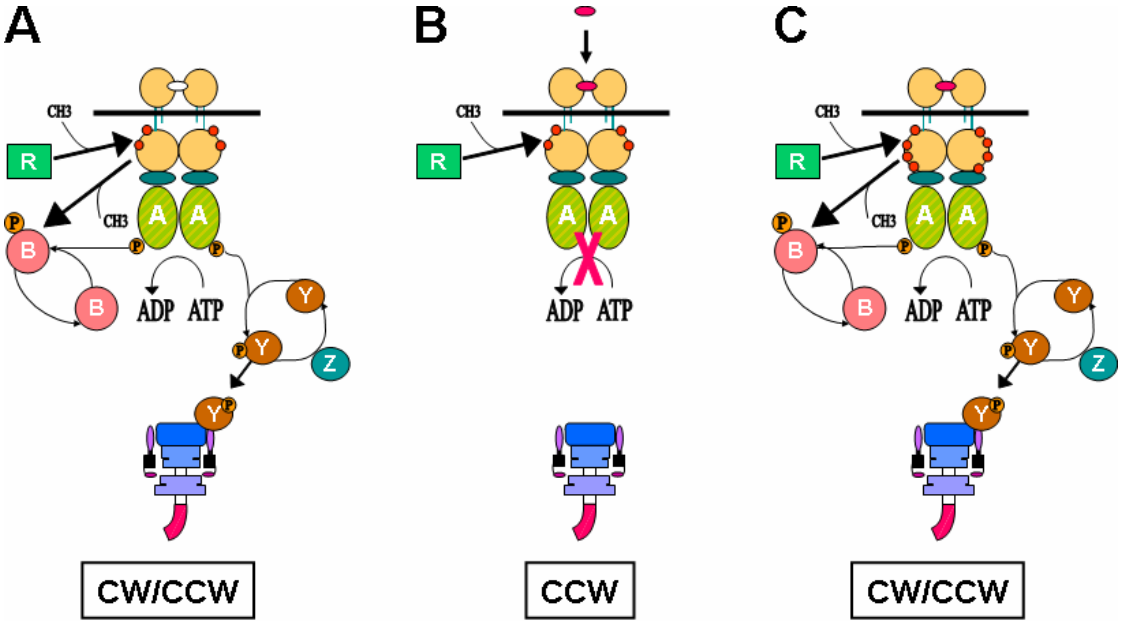

Figure 1.2. The chemotactic circuit underlying control of flagellar rotation. (A) In the absence of chemoeffectors, baseline CheA activity maintains phospho-CheY levels produce a random walk as depicted in Figure 1.1B. (B) Binding of attractant to the chemoreceptor abolishes CheA stimulation, thereby decreasing intracellular phospho-CheY levels. This reduces the probability of a tumbling event and biases the random walk as depicted in Figure 1.1C. (C) Adaptive methylation restores the ability of the receptor to stimulate CheA activity when the receptor is occupied by an attractant ligand. These antagonistic activities allow the cell to compare the current environment to one from a few seconds earlier.

Chemoreceptors combine several allosteric inputs to generate a single output

A chemoreceptor must process various allosteric inputs, such as ligand occupancy, covalent modification, protein-protein interactions, and protein-membrane interactions, into a single signal output (kinase modulation) (Figure 1.3A). The cytoplasmic signaling subdomain that interacts with CheW and the CheA kinase is a coiled-coil of two antiparallel helices. Within a homodimer, two coiled-coils form a four-helix bundle (*28*) (Figure 1.3B). The "frozen dynamic" model for modulation of CheA activity (*29, 30*) suggests that allosteric inputs change the supercoiling state of this four-helix bundle. In the "off" (attractant-bound) state, the receptor has more conformational freedom, whereas in the "on" (repellent-bound) state the four-helix bundle is less dynamic. The "on" state is hypothesized to stimulate CheA activity by allowing the four-helix bundle to spend more time in a conformation with high affinity for CheA and CheW (*31*). Each class of allosteric input is considered below within the context of the frozen dynamic model.

Transmembrane signaling in response to chemoeffectors

Tar functions as the aspartate and maltose chemoreceptor in *E. coli* (*32*). Aspartate or maltose coverts Tar from a stimulator of kinase activity to an inhibitor (*20*). Aspartate binds directly to Tar, but signaling in response to maltose requires maltose-binding protein (MBP), which is a member of the bacterial periplasmic binding protein (bPBP) superfamily (*33*). Ligand-free MBP exists in equilibrium between the "open" and "closed" conformations (*34*). Maltose binding shifts the equilibrium toward the

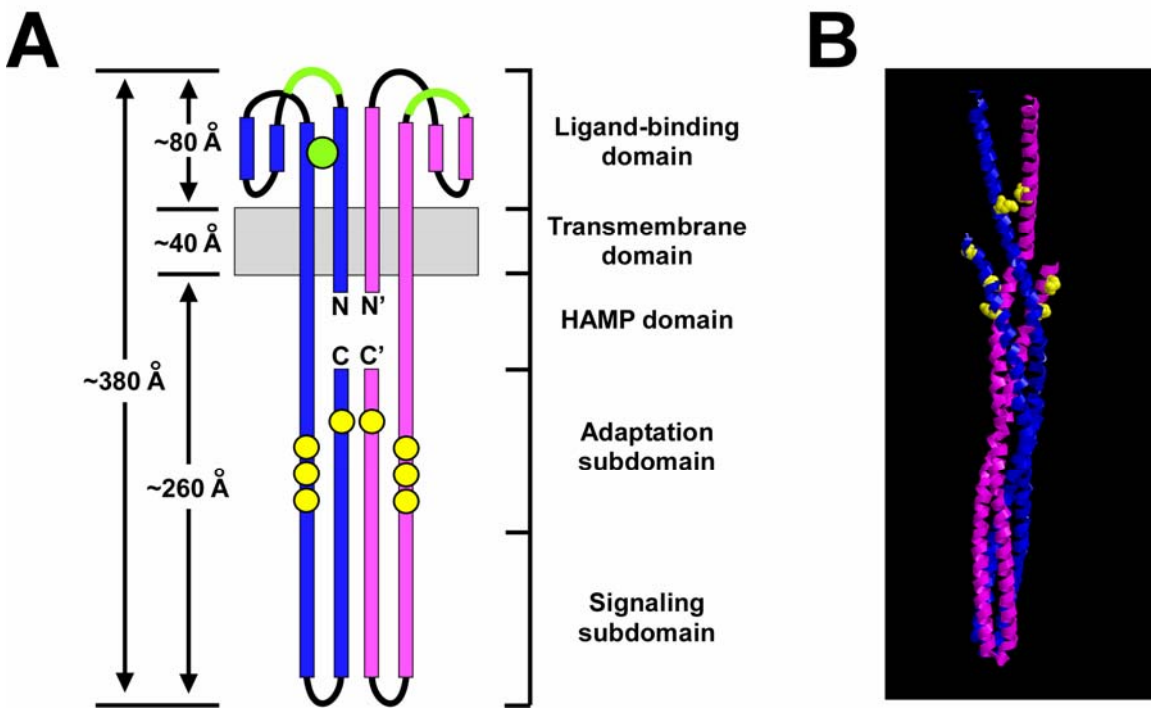

Figure 1.3. Domain structure of homodimeric Tar. (A) A topological representation of the homodimeric *E. coli* Tar chemoreceptor. The periplasmic portion of the receptor consists of the ligand-binding domain that interacts with aspartate and ligand-bound maltose-binding protein (MBP). One aspartate binding site and one docking site for ligand-bound MBP are represented in green. The cytoplasmic domain consists of the HAMP domain and the adaptation and signaling subdomains. The four sites of covalent modification within each monomer are depicted as yellow dots. (B) The adaptation and signaling subdomains of Tar are composed of a coiled-coil formed from contiguous antiparallel α helices connected by a U-turn within each monomer (*28*). Within a homodimer these coiled-coils form a four-helix bundle. The sites of covalent modification are depicted in yellow space-filling models. The frozen dynamic model (*29*) suggests that allosteric effectors modulate the conformational dynamics of the four-helix bundle within the signaling subdomain. Reduced conformational dynamics results in a greater percentage of time spent in conformations that interact with CheA and CheW with high affinity.

"closed" conformation, in which it interacts with the apical loops of the periplasmic domain of Tar (*35-37*). Tar is unusual because the periplasmic domain interacts both with small ligands such as aspartate and with a ligand-bound binding protein. The transmembrane conformational change triggered by these interactions is well-characterized (*38-44*) and currently serves as the paradigm for other chemoreceptors, and potentially also for numerous members of the homodimeric sensor histidine kinase superfamily (*45*). Tar also mediates repellent responses to divalent cations (Ni^{2+} and Co^{2+}) (2), although the binding sites and the signaling mechanisms are not understood.

The crystal structures of the periplasmic domains of Tar from *Salmonella enterica* serovar Typhimurium (*35, 46*) and *E. coli* (*47*) show that each monomeric unit of the functional homodimer (*48, 49*) consists of four antiparallel α helices that form a quasi four-helix bundle (Figure 1.4A). Studies of sulfhydryl reactivity demonstrate that the transmembrane regions (TM1 and TM2) flanking the periplasmic domain of Tar are extensions of the periplasmic helices H1 and H4 (*50-55*) (Figure 1.4B). Aspartate binds at either of two rotationally symmetric sites at the dimer interface, each of which contains residues from H1 and H4 of one subunit and H1' of the opposing subunit (*46*). *E. coli* Tar exhibits "half-of-sites" binding such that, under physiological conditions, only one molecule of aspartate associates with a given dimer (*56*). Aspartate binding generates a downward vertical displacement of a few angstroms in one H4-TM2 helix relative to its H1-TM1 helix partner (*38, 40-44*) (Figure 1.4B). Trg, another *E. coli* chemoreceptor that interacts with ligand-bound ribose-binding protein (RBP) and glucose/galactose-binding protein (GGBP), seems to share a similar mechanism of

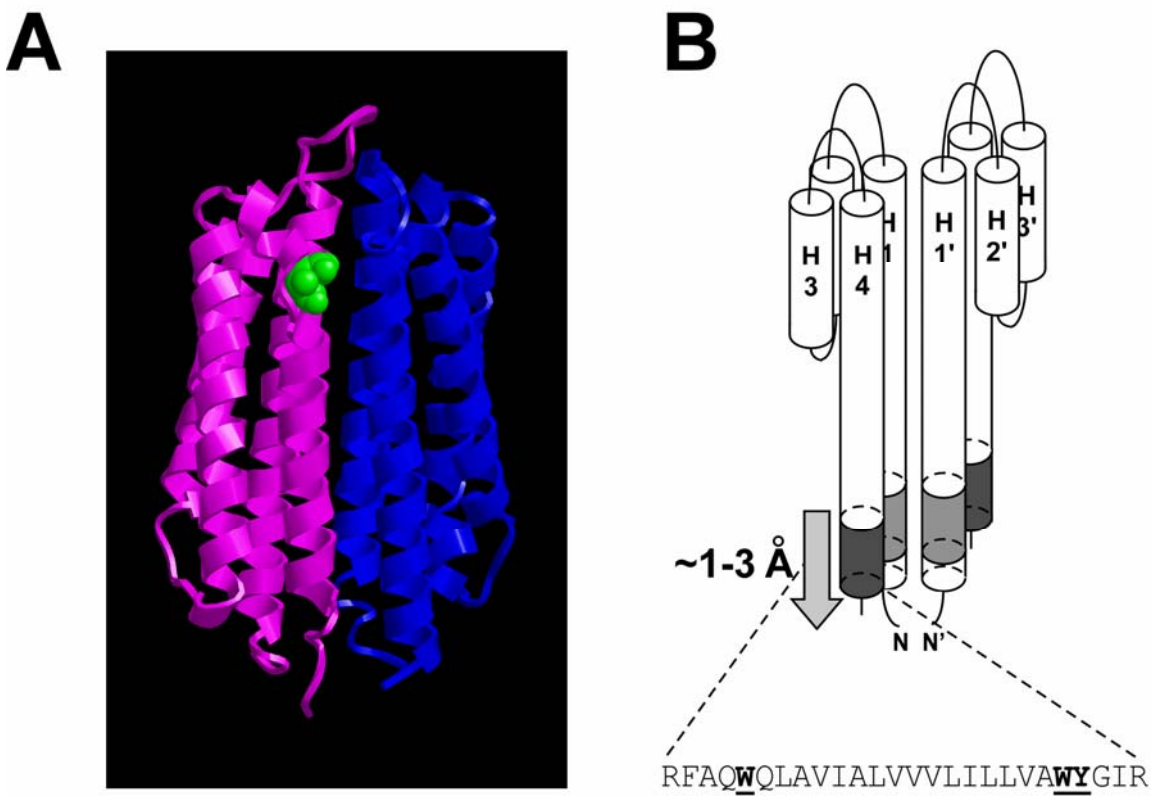

Figure 1.4. Structure of the periplasmic domain of Tar. (A) Three-dimensional structure of the ligand-bound conformation of homodimeric *S. typhimurium* Tar (*35*, *46*). A single aspartate molecule is represented as a green spacefilling model. (B) Schematic representation of the periplasmic and transmembrane (TM) domains of the *E. coli* Tar chemoreceptor. TM1 and TM2 are represented as light and dark shaded areas, respectively. Upon binding aspartate, TM2 of one monomer (*54*, *55*) is proposed to be displaced toward the cytoplasm, thereby repositioning TM2 relative to the phospholipid bilayer. The extent of TM2 shown is based on sulfhydryl-reactivity studies with 5-IAF and *S. typhimurium* Tar (*42*). The locations of the Trp-192, Trp-209, and Tyr-210 residues, which are predicted to reside at the polar-hydrophobic interfacial regions of the cytoplasmic membrane, are emphasized.

transmembrane signaling when ligand-bound bPBPs interact with it (*39*). In both cases, this "piston" movement repositions TM2 relative to the plane of the cell membrane, thereby conveying the presence of attractants to the interior of the cell.

Two models for signal processing by the HAMP domain

The HAMP domain functions as a linker between the periplasmic and cytoplasmic domains of Tar. It physically connects TM2 to the adaptation subdomain (Figure 1.3A). It somehow converts vertical displacements of TM2 (*38, 40-44*) into changes in the helical supercoiling of the adaptation and signaling subdomains (*28-30, 57*). The HAMP domain consists of two amphipathic helices (AS1 and AS2) connected by a short flexible linker (*58-60*). Binding of attractants to the periplasmic domain of Tar is predicted to increase conformational dynamism in the signaling subdomain, resulting in decreased kinase stimulation (*29*). Currently, two possible mechanisms for conversion of a piston-type displacement into altered supercoiling have been proposed (*60, 61*).

The first model proposes a major transition from one conformation of the HAMP domain to another (Figure 1.5A). In the absence of attractant, the HAMP domain might reduce the conformational dynamics of the adaptation and signaling subdomains by forming an AS2-AS2' coiled-coil domain, as suggested by sulfhydryl-reactivity studies (*58*). The "helix interaction model" proposes that AS1 lies parallel to the membrane (*60*). The plausibility of this idea is supported by a recent survey of high-resolution structures of integral membrane proteins (*62*). Interaction with attractants, by displacing TM2 toward the cytoplasm, could decrease AS1-membrane interactions. Instead of TM2

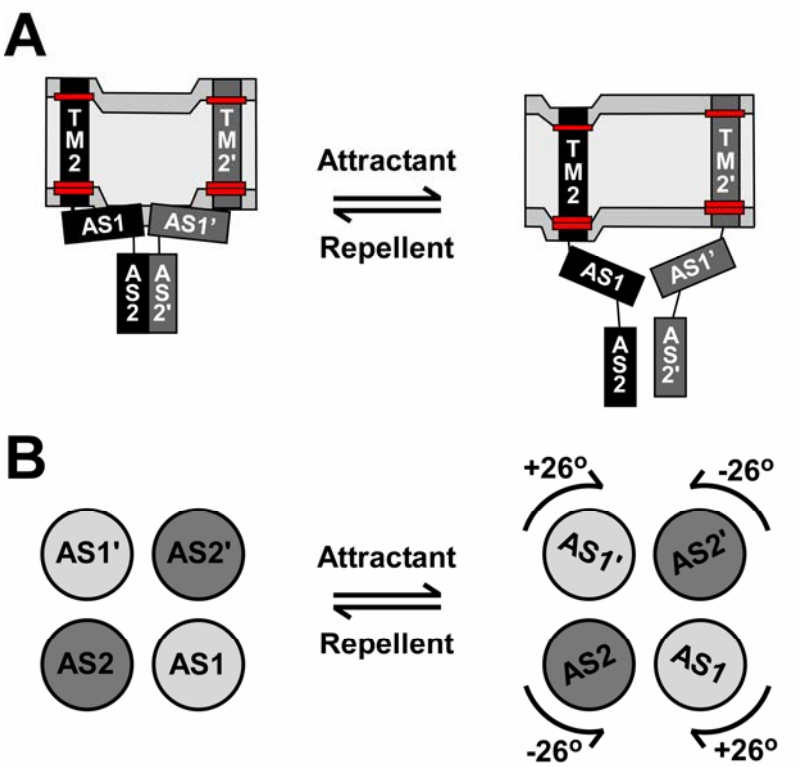

Figure 1.5. Two models for function of the HAMP domain. (A) The "helix interaction" model (*60*) suggests that aspartate binding displaces TM2 and produces a localized membrane deformation because of the affinity of the amphipathic aromatic residues (red boxes) for the polar-hydrophobic interfaces. Note that only one TM2 is displaced, to account for the asymmetric attractant-induced signaling (*54*, *55*). This distortion would decrease the affinity of AS1 for the membrane and produce another interaction surface for AS2 or AS2'. A decrease (right side) in AS2-AS2' interactions diminishes supercoiling (increased spacing between AS2 and AS2') of the adaptation and signaling subdomains shifting the equilibrium toward "off" (to the right). Presumably, repellents displace TM2 toward the periplasm, which should increase AS1-membrane affinity and promote AS2-AS2' interactions (decreased AS2-AS2' spacing), shifting the equilibrium toward the "on" state (to the left). (B) Based on the solution structure of a HAMP domain, the other model (*61*) suggests that no large-scale changes in helical pairing occur. Changes in the supercoiling of the adaptation and signaling subdomains are mediated by interhelical rotation between AS2 and AS2'. This model requires no TM2 displacement relative to the membrane or interactions of the HAMP domain with the inner leaflet of the membrane.

being displaced out of the plane of the membrane into aqueous solution, which would be energetically unfavorable, it is possible that the displacement results in a localized membrane deformation due to affinity of the amphipathic aromatic residues for the polar-hydrophobic interfacial regions (*63, 64*). This localized distortion could reduce the affinity of AS1 for the membrane surface. Freeing AS1 from the membrane would, in turn, create another hydrophobic interaction surface for AS2, thereby shifting the equilibrium away from the stabilizing AS2-AS2' coiled-coil.

The second model is based on a solution structure of a purified hyperthermophilic HAMP domain (*61*) that suggests a 26º helical rotation of α helices within a parallel coiled-coil is responsible for generating changes in supercoiling of the signaling subdomain (Figure 1.5B). This model implies that vertical displacement of TM2 relative to the membrane is not essential for signal transduction by the HAMP domain. The conditions required to generate the structural information may limit its generality. First, potential interactions with the membrane are absent because solution NMR was used to generate the structural data. Secondly, the HAMP domain used was atypical because it came from an archaeal receptor that contained no other cytoplasmic subdomains. Critical examination of potential HAMP-membrane interactions could be used to differentiate between these possibilities and will be discussed in Chapter IV. It remains an interesting possibility that the structure determined represents one particular conformation of all HAMP domains, perhaps in the "off" state.

Methylation modulates the conformational dynamics of the adaptation subdomain

Following the HAMP linker, the remainder of the cytoplasmic domain forms an extended four-helix bundle consisting of antiparallel alpha helices from each monomer (Figure 1.3). The membrane-proximal portion of the adaptation subdomain is an extension of AS2 from the HAMP domain, whereas the membrane-distal portion forms a topologically contiguous four-helix bundle with the signaling subdomain (*28, 65*) (Figure 1.3B). Four glutamyl residues within each monomer are subject to covalent modification by the CheR methyltransferase (*22*). *In vitro* analyses in which the negative charges of these residues were neutralized, corresponding to methylation, reduced electrostatic repulsion between the two subunits of a homodimer and increased kinase stimulation. These results support the frozen dynamic model because the adaptation subdomain is a direct extension of the signaling subdomain. Reduced electrostatic repulsion would be expected to reduce the conformational dynamics of the signaling subdomain (*66, 67*).

Higher-order interactions with other chemoreceptors promote signal integration

Ligand occupancy and covalent modification are predicted to alter the conformational dynamics of signaling subdomains within individual homodimeric chemoreceptors as described above. However, under most conditions, *E. coli* cells will encounter multiple external stimuli. To determine an appropriate behavioral response, the signals sensed by different chemoreceptors must be processed into an integrated output.

The fundamental level of organization responsible for signal processing and integration is a trimer of chemoreceptor dimers (*28*). In this structure, three chemoreceptor homodimers interact within their membrane-distal signaling subdomains. These trimers of dimers can be composed of different homodimeric chemoreceptors (*68-71*), an arrangement that enhances the processing of multiple detection events. These interactions are also likely to account for the exquisite sensitivity of the chemosensing machinery (*14*) and the positive cooperativity observed during titration of kinase-stimulating activity with attractants (*25, 26, 43, 71-73*).

A final level of spatial organization is required for proper signal processing. Repeating receptor-CheA-CheW complexes are believed to form large patches containing thousands of receptors that are localized to the poles of the cell (*74-76*). The remaining chemotaxis proteins also localize to these patches via interaction with the receptor (CheR and CheB) or interaction with CheA (CheB, CheY, and CheZ) (*77*). Therefore, the efficient processing of various allosteric inputs into a single decision by the cell requires multiple levels of organizational hierarchy, ranging from the formation of individual chemoreceptor dimers to large-scale cellular localization of chemosensory patches.

The role of protein-membrane interactions during transmembrane signaling

Any membrane-spanning receptor that detects extracellular stimuli must transduce that information to the interior of the cell. As discussed earlier, the mechanism of signal transduction across the cellular membrane involves displacement of TM2 a few

angstroms toward the cytoplasm (*38-44*). This displacement repositions a dynamic transmembrane helix relative to the plane of lipid bilayer, thereby constituting another class of allosteric effectors that must be examined.

Phospholipid bilayers consist of polar, hydrophilic regions that flank a central nonpolar, hydrophobic core. The acyl chains that form the hydrophobic core account for approximately half the total bilayer thickness. The remainder is composed of the two flanking polar regions that contain the hydrophilic phosopholipid headgroups (*78*). To minimize energetically unfavorable protein-membrane interactions, certain amino acyl residues are usually located at different positions within a membrane-spanning α helix. Comparison of three-dimensional structures of integral membrane proteins and sequence analysis of predicted transmembrane α helices suggest a common motif in which a central core of aliphatic residues is flanked by amphipathic aromatic residues at the polar-hydrophobic interface and charged residues at the membrane-water interface (*79*). The primary sequence of TM2 of *E. coli* Tar conforms to this motif (*42*) (Figure 1.4).

Several lines of evidence demonstrate that amphipathic aromatic residues in transmembrane helices are significant determinants in governing how a transmembrane helix interacts with the membrane. A glycosylation-site mapping technique (*80*) implicated Trp residues in determining the vertical position of a synthetic poly-Leu transmembrane α helix oriented roughly perpendicular to the membrane. Shifting the location of Trp residues within the peptide repositioned the α helix to allow Trp to reside within the interfacial zone (*63*). In addition, synthetic peptides consisting of an Ala-Leu core of different lengths flanked by Trp (WALP peptides) (*81*) interact in a characteristic

manner with phospholipid bilayers. The flanking Trp residues exhibit a very strong tendency to remain within the interfacial region regardless of the length of hydrophobic mismatch (*64*). Hydrophobic mismatch occurs when the length of the aliphathic residues within a transmembrane helix is different than the thickness of the hydrophobic core of the lipid bilayer it passes through. Previously, hydrophobic mismatch was thought to be the dominant element in determining how transmembrane helices interact with their lipid environment. This result demonstrates that Trp residues play a more significant role in positioning α helices within a membrane.

Dissertation overview

The research presented within this dissertation investigates the role of receptor-membrane interactions, specifically the contribution of Trp residues flanking TM2, in maintaining the baseline signaling state of *E. coli* Tar. The study presented in Chapter II thoroughly examined the contribution of these residues. The presence of Trp-209 was found to be essential, whereas substitution of Trp-192 did not significantly alter the signaling state of Tar. Substitution of Ala for Trp-209 abolished *in vitro* kinase stimulation and severely biased the baseline signaling output toward the ligand-bound conformation *in vivo*. Tyr-210 was found to play an auxiliary role in maintenance of signal output.

Chapter III demonstrates that the interactions between TM2 and the membrane can be harnessed to modulate the signaling state of *E. coli* Tar. The baseline signaling state of Tar was incrementally altered by repositioning the Trp-209/Tyr-210 pair about

their original position. Moving these residues is predicted to reposition TM2 within the membrane to modulate signaling output. To my knowledge, this is the first published example (*44*) of harnessing membrane-protein interactions to modulate the signal output of a transmembrane receptor predictably and incrementally.

Potential future extensions of this research are discussed in Chapter IV. These include identification of HAMP-membrane interactions to differentiate between the proposed mechanisms for signal propagation and the use of analogous mutations in the sensors of the two-component signaling pathways that are ubiquitous in prokaryotes.

CHAPTER II

TRYPTOPHAN RESIDUES FLANKING THE SECOND TRANSMEMBRANE DOMAIN (TM2) SET THE SIGNALING STATE OF THE TAR CHEMORECEPTOR*

Overview

This chapter is a published work (*43*). It assesses the contribution of the tryptophan residues flanking the second transmembrane domain (TM2) to maintenance of the basal signaling state of the aspartate chemoreceptor (Tar) of *Escherichia coli*. I conceived and conducted the majority of the experimentation described within this chapter. Dr. Arjan F. Bormans established the protocol for determining the extent of methylation *in vivo* and performed the experiments described in Figures 2.2 and 2.3. Dr. Run-zhi Lai and I worked together to establish the protocol and purify the proteins necessary for the receptor-coupled *in vitro* phosphorylation assay used in Figure 2.1 and Tables 2.2 and 2.4.

Summary

The chemoreceptors of *Escherichia coli* are homodimeric membrane proteins that cluster in patches near the cell poles. They convert environmental stimuli into intracellular signals that control flagellar rotation. The functional domains of a receptor

---

*****Reproduced with permission from "Tryptophan residues flanking the second transmembrane domain (TM2) set the signaling state of the Tar chemoreceptor" by Draheim, R. R., Bormans, A. F., Lai, R.-Z., and Manson, M. D., 2005, *Biochemistry 44,* 1268-77. Copyright 2005 American Chemical Society.

are physically separated by the cell membrane. Chemoeffectors bind to the extracellular (periplasmic) domain, and the cytoplasmic domain mediates signaling and adaptation. These two domains communicate through the second transmembrane helix (TM2) that connects them. In the high-abundance receptors Tar and Tsr, TM2 is flanked by tryptophan residues, which should localize preferentially to the interfacial zone between the polar and hydrophobic layers of the phospholipid bilayer. To investigate the functional significance of the Trp residues that flank TM2 of Tar, we used site-directed mutagenesis to generate the W192A and W209A substitutions. The W192A protein retains full activity *in vivo* and *in vitro*, but it increases the K_i for aspartate in the *in vitro* assay 3-fold. The W209A replacement eliminates receptor-mediated stimulation of CheA *in vitro*, and it leads to an increased level of adaptive methylation *in vivo*. This W209A substitution may cause the C-terminus of TM2 to protrude farther into the cytoplasm, these results reinforce the hypothesis that aspartate binding causes a similar displacement. Moving Trp to each position from residue 206 to residue 212 generated a wide variety of Tar signaling states that are generally consistent with the predictions of the piston model of transmembrane signaling. None of these receptors was completely locked in one signaling mode, although most showed pronounced signaling biases. Our findings suggest that the Trp residues flanking TM2, especially Trp-209, are important in setting the baseline activity and ligand sensitivity of the Tar receptor. We also conclude that the Tyr-210 residue plays at least an auxiliary role in this control.

Introduction

Escherichia coli performs chemotactic migrations in response to a wide variety of environmental stimuli, including changes in pH (*2*), temperature (*82*), redox potential (*3*, *4*), amino acids (*5*), sugars (*6*), small peptides (*7*), and certain noxious organic compounds and divalent cations (*2*). Cells swim up gradients of attractant stimuli and down gradients of repellent ones. To do so, cells bias a three-dimensional random walk of alternating smooth swims (runs) and reorienting tumbles by selectively lengthening runs in the favorable direction (*12-14*).

The signal transduction pathway that directs the biased random walk controls the direction of flagellar rotation. Each of the five members of a family of homodimeric chemoreceptors detects a specific set of stimuli. These receptors normally activate the histidine protein kinase CheA (*15*), which is coupled to the receptors via the adapter protein CheW. CheA autophosphorylates, and the phosphoryl group is then transferred to the response regulator CheY (*16*). CheY-P binds to FliM in the flagellar motor to promote clockwise (CW) rotation of the flagella (*17*, *18*). Counterclockwise (CCW) motor rotation allows the flagellar filaments, which are left-handed helices, to coalesce into a bundle that propels the cell in a run (*10*). CW rotation of one or more flagella disrupts the bundle and generates a tumble (*11*). The relative activities of CheA and the CheY-P phosphatase, CheZ, establish the ratio of CheY to CheY-P within the cell, and hence the frequency of tumbling (*15*, *19*).

The conformational changes induced by an attractant stimulus convert a receptor from a stimulator of CheA activity into an inhibitor (*20*). The resulting drop in CheY-P,

which is accelerated by CheZ, suppresses tumbling and lengthens the average run. Inhibition of CheA activity is reversed by covalent methylation of the cognate receptor (*21*). Methylation is also facilitated by a transient decrease in the level of the active, phosphorylated form of the CheB methylesterase (*24*), which is another substrate for phosphotransfer from CheA (*16*).

Tar functions as the aspartate chemoreceptor in *E. coli* (*32*). The crystal structures of the periplasmic ligand-binding domains of Tar from *Salmonella enterica* serovar Typhimurium (*35, 46*) and *E. coli* (*47*) show that each monomeric unit of the functional homodimer (*48*, *49*) consists of four antiparallel α helices that form a quasi four-helix bundle. Sulfhydryl reactivity experiments (*50-53*) demonstrate that the transmembrane regions (TM1 and TM2) flanking the periplasmic domain are extensions of the periplasmic helices H1 and H4. Aspartate binds at either of two rotationally symmetrical sites at the dimer interface, each of which contains residues from H1 of one subunit and H4 of the opposing subunit. *E. coli* Tar exhibits half-of-sites binding such that, under most conditions, only one molecule at a time of aspartate associates with a given dimer (*56*). Aspartate binding is proposed to generate a downward vertical displacement of a few angstroms in one H4-TM2 helix relative to its H1-TM1 helix partner (*38*, *40-44*). This movement should also reposition TM2 relative to the plane of the cell membrane. Tryptophan residues in transmembrane helices localize preferentially to the interfacial regions of phospholipid bilayers (*83*). A glycosylation-site mapping technique (*80*) implicated Trp residues in determining the vertical position of a synthetic poly-Leu transmembrane helix oriented roughly perpendicular to the membrane. Shifting

the location of Trp residues within the peptide repositioned the helix to allow Trp to reside within the interfacial zone (*63*). Also, synthetic peptides consisting of an Ala-Leu core of different lengths flanked by Trp (WALP peptides) interact in a characteristic manner with phospholipid bilayers (*81*). The flanking Trp residues exhibit a strong tendency to remain within the interfacial region regardless of the length of hydrophobic mismatch (*64*), indicating that they are significant determinants in governing how a transmembrane helix interacts with the membrane.

TM2 of *E. coli* Tar consists of a largely aliphatic core of sixteen residues bounded by a Trp residue at each end. It thus resembles a WALP peptide. This striking similarity prompted us to examine whether these Trp residues modulate the signaling state of Tar. We report here the effects of the residue substitutions W192A and W209A on the function of Tar *in vivo* and *in vitro*. We then describe the results obtained when Trp was moved from position 209 to each of positions 206 through 212. Our findings emphasize the crucial role of Trp-209 in regulating the activity of the Tar receptor. By extension, they suggest that the aromatic residues that are conserved in many homodimeric chemoreceptors and transmembrane sensor kinases may play a similarly important role. Finally, we propose that our results support a piston model for transmembrane signaling by this entire set of bacterial proteins.

Materials and methods

Bacterial strains and plasmids

Strain RP3098 (*84*) is a Δ*(flhD-flhB)4* derivative of the *E. coli* K-12 strain RP437 (*85*). Strain VB13 (*86*) is a *thr*+ *eda*+ Δ*tsr7201 trg*::Tn*10* Δ*tar-tap5201* version of RP437. Plasmid pRD100 was created by cloning the PCR-amplified *tar* gene from plasmid pMK113 (*87*) into pBAD18 (*88*), using flanking *Eco*RI and *Hin*dIII restriction sites. Plasmid pRD200 was made by adding an in-frame coding sequence to the 3′ end of *tar*. This sequence encodes a seven-residue linker (GGSSAAG) (*89*) and a C-terminal V5 epitope tag (GKPIPNPLLGLDST) (*90*). The *Bam*HI site in the *tar* promoter region of pMK113 was also removed to restore the wild-type sequence. Plasmid pRD300 is identical to pRD100 except for the addition of the in-frame coding sequence for the seven-residue linker and C-terminal V5 tag. Mutations were introduced into *tar* in these plasmids using standard site-directed mutagenesis techniques (Stratagene).

Observation of swimming cells

Cells were inoculated from a single colony on Luria Broth agar (*91*) containing 50 μg/mL ampicillin into 25 mL of tryptone broth (*91*) supplemented with 50 μg/mL ampicillin. Cultures were swirled at 32 °C until they reached an optical density at 600nm of ~0.7, at which time a large majority of cells were highly motile. Cells were diluted 1:50 into tethering buffer [10 mM potassium phosphate (pH 7.0), 100 mM NaCl, 10 μM EDTA, 20 μM L-methionine, 20 mM sodium lactate, 20 μg/mL chloramphenicol] and observed at 1000× magnification under phase contrast using an oil immersion 100×

objective and Olympus BH-2 microscope. Ten separate fields, each traversed by five to ten cells during the approximately 30 s observation period, were analyzed for each strain. A subjective assessment was made of whether individual cells were running and tumbling (R cells), smooth swimming (S cells), or primarily tumbling (T cells).

Observation of tethered cells

Cultures were grown as described above and harvested by centrifugation after the addition of chloramphenicol to a final concentration of 30 μg/mL to prevent regrowth of flagella after shearing. Cells were resuspended in 25 mL of tethering buffer containing 30 μg/mL chloramphenicol and exposed to six 10-s intervals of agitation at high speed in a 50 mL stainless steel cup of a Waring blender. Bouts of blending were separated by 15 s to allow cooling. Cells were then pelleted by centrifugation and resuspended in 5 mL of tethering buffer containing chloramphenicol. These cells were kept on ice until needed, when 20 μL of cell suspension was mixed with 20 μL of a 200-fold dilution of anti-flagellar filament antibody. This entire volume was loaded within a peripheral ring of Apiezon-L grease on a 12 mm diameter round coverslip. After incubation for 20 min at room temperature, coverslips were affixed to a flow chamber (*92*), and nontethered cells were removed by passing several milliliters of tethering buffer through the chamber. Cells were observed at 1000× magnification, as described above. Enough fields were videotaped for ~1 min apiece to ensure that at least 30 freely rotating cells could be analyzed for each strain. Rotational behavior was assessed during video playback. Cells were divided into three categories: cells that turned their flagella only

CCW, cells that exhibited only a few, brief reversals to CW flagellar rotation, and cells that reversed often and/or rotated for extended intervals both CCW and CW.

Chemotaxis swarm assays

Swarm assays were run as described (*89*), with minor modifications. Briefly, semisolid agar contained 0.325 g/L Difco BactoAgar in motility medium [10 mM potassium phosphate (pH 7.0), 1 mM $(NH_4)_2SO_4$, 1 mM $MgSO_4$, 1 mM $MgCl_2$, 1 mM glycerol, 90 mM NaCl] supplemented with 20 μg/mL L-threonine, L-histidine, L-methionine, and L-leucine and 1 μg/mL thiamine. Ampicillin was present at 25 μg/mL. Aspartate and maltose were added to a final concentration of 100 μM. Swarm plates were incubated at 30 °C. Once visible swarm rings formed, their diameter was measured every 2 h, and the rate of ring expansion was expressed in mm/h.

Protein preparation

We employed the protocol of Gegner et al. (*93*), with minor modifications. Strain RP3098 containing pRD100 or one of its derivatives was used for production of receptor-containing membranes. Tar expression was induced by addition of L-arabinose to a final concentration of 0.2% (w/v). CheY was purified using the method described by Hess et al. (*94*).

Receptor-linked CheA kinase assay

We employed a slightly modified version of the receptor-coupled phosphorylation assay described by Borkovich and Simon (*95*). Tar containing membranes (20 pmol of Tar) and CheY (500 pmol) were added to CheA (5 pmol) and CheW (20 pmol), which were incubated overnight on ice in a total volume of 9 μL of fresh phosphorylation buffer [50 mM Tris-HCl, 50 mM KCl, 5 mM $MgCl_2$, 2 mM DTT (pH 7.5)]. Aspartate was added to the desired final concentration while the same total volume was maintained. This mixture was then held at room temperature for 4 h. The reaction was initiated by addition of 1 μL of [γ-^{32}P]-ATP (3000 Ci/mmol NEN# BLU502A) diluted 1:1 with 10 mM unlabeled ATP. Reactions were terminated by adding 40 μL of 2X SDS-PAGE loading buffer containing 25 mM EDTA. Production of CheY-^{32}P was determined to be linear through 20 s and to be proportional to the amount of receptor present over a range from 5 to 40 pmol (data not shown). Ultimately, we used 20 pmol in each reaction because this concentration is in the middle of the linear range, allowing us to measure increases or decreases in production of CheY-P accurately. Analysis of the aspartate-induced titration curves was performed according to a previously described method (*25*), using KaleidaGraph v3.6 software and the Hill equation to determine the cooperativity of inhibition by aspartate. We calculated the concentration of free aspartate by performing a series of iterations in which we used the uncorrected aspartate values to determine an approximate K_i, which was then used to determine free aspartate (total minus bound) to calculate a new K_i. We performed consecutive iterations until no change in K_i or the Hill coefficient was observed. The

uncertainties in the estimates of the K_i and Hill coefficients represent the standard deviation of the mean, with $n \geq 3$.

Determination of the methylation state of receptors in vivo

We adapted our methylation assay from Weerasuriya et al. (*86*). To determine levels of receptor methylation, VB13 cells harboring plasmid pRD200 or one of its mutant derivatives were grown to an OD_{590nm} of 0.6 in 10 mL of tryptone broth (*91*). Cells were harvested by centrifugation and washed three times with 10 mM potassium phosphate, 0.1 mM EDTA (pH 7.0) and finally resuspended in 5 mL of 10 mM potassium phosphate (pH 7.0), 10 mM sodium lactate, and 200 μg/mL chloramphenicol. One-milliliter aliquots of cells were transferred to 10-mL scintillation vials and incubated with shaking for 10 min at 32 °C. Following addition of L-methionine to 2 μM, cells were incubated for an additional 30 min. In some samples, aspartate or $NiSO_4$ was added to 100 mM and 10 mM, respectively, and the cells were incubated for an additional 20 min. Control reactions received an equal volume of buffer. Reactions were terminated by addition of 100 μL of ice-cold 100% TCA and then incubated on ice for 15 min. Proteins were pelleted by centrifugation at 13000*g* and subsequently washed with 1% TCA and acetone. The proteins were resuspended in 200 μL of 2X SDS-loading buffer. A 10-μL aliquot of each sample was loaded into a 7.5% SDS gel. Following electrophoresis, the proteins were transferred to nitrocellulose and subjected to immunoblotting and visual detection by antibody against the V5 epitope (Invitrogen),

using goat anti-mouse conjugated with alkaline phosphatase (Bio-Rad) as the secondary antibody.

Results

Substitution of Trp residues flanking TM2 with Ala

The position of TM2 of Tar relative to TM1 is a crucial factor in transmembrane signal transduction (*38-44*). Inspired by the demonstrated role of Trp residues in positioning transmembrane helices, we decided to assess the role of the Trp-192 and Trp-209 residues that flank TM2 in modulating the signaling state of the receptor (Figure 1.4B). We generated mutant versions of Tar containing the W192A or W209A substitution as well as the W192A-W209A (WAWA) double substitution. We chose Ala as the replacement residue because it removes the amphipathic character of Trp, does not introduce charge or polar character, and minimizes the probability of introducing steric hindrance or helix disruption. We made these changes in plasmid pRD200, which expresses fully functional Tar with a C-terminal V5 epitope tag (see below).

Chemotactic behavior of cells expressing Trp-substituted receptors

We expressed both wild-type and mutant Tar proteins in the transducer-depleted (ΔT) strain VB13, which retains the redox receptor Aer. The chemotactic behavior of these cells was tested in aspartate, maltose, and glycerol motility agar, the last of which allows an assessment of aerotaxis in the absence of any specific Tar chemoeffector. Substitution of Trp-192 with Ala decreased the rate of swarm-ring expansion in aspartate

and maltose motility agar to 85% of the wild-type rate, a statistically insignificant difference (Table 2.1). In contrast, substitution of Trp-209 with Ala decreased the rate of ring migration to 45% and 60% of the wild-type rate in aspartate and maltose semisolid agar, respectively. When both Trp-192 and Trp-209 were substituted with Ala, intermediate expansion rates of 60% and 70% of the wild-type rate were observed. All mutants formed aerotaxis rings in agar containing only glycerol, with swarms expanding at 85%, 70%, and 80% of the wild-type rate for the W192A, W209A, and WAWA mutants, respectively.

The swarms made by cells expressing either W209A or WAWA Tar formed significantly sharper rings on aspartate plates (data not shown). This result suggests that these cells may respond differently to the aspartate gradient produced by the expanding colony.

Stimulation of CheA activity by Trp-substituted receptors in vitro

Any inherent changes in the ability of the mutant receptors to stimulate CheA activity or to alter their activity in response to aspartate could be partially masked by adaptive methylation. Performing *in vitro* assays using purified components in the absence of CheR and CheB avoids this complication. We therefore isolated inner-membrane vesicles from cells in which wild-type or mutant Tar proteins were expressed at high levels from an arabinose-inducible, plasmid-borne *tar* gene in strain RP3098, which lacks all flagellar, motility, and chemotaxis proteins. These membranes were then used in an in vitro assay for receptor-coupled CheA kinase activity (*95*). In these

Table 2.1: Swarm behavior of cells harboring the Trp-to-Ala Tar proteins.

	Swarm expansion rates[a]		
Receptor	Aspartate	Maltose	Glycerol
WT	1.72 ± 0.14	0.87 ± 0.04	0.55 ± 0.04
W192A	1.49 ± 0.11	0.71 ± 0.10	0.46 ± 0.05
W209A	0.67 ± 0.00	0.50 ± 0.03	0.38 ± 0.01
WAWA	0.48 ± 0.07	0.57 ± 0.09	0.43 ± 0.03

[a] The rate at which the swarm diameter increased was measured in mm/hr, as described in Materials and Methods. The error represents the standard deviation of three independent assays.

membranes, all of the Tar present is in the unmodified state in which the protein is originally translated. The four sites of covalent methylation are correspondingly occupied by two Gln residues and two Glu residues (the QEQE form of the receptor). Tar constituted between 50% and 65% of the total protein in membrane preparations for the wild-type and mutant receptors (data not shown). Thus, all of the mutant proteins are reasonably stable.

Receptor/CheA/CheW complexes containing wild-type Tar produced produced 44 ± 1 pmol of CheY-P in 20 s (Table 2.2). Complexes containing the W192A mutant Tar produced 44 ± 6 pmol in 20 s, similar to the wild-type receptor. The W209A substitution, either by itself or in combination with W192A, eliminated receptor-mediated stimulation of CheA activity almost completely. This behavior resembles that of the previously described "lock-off" disulfide-scanning mutants (*38*), in which no modulation of CheA activity was detected. We concluded that the relatively good swarming of cells expressing Tar W209A or WAWA might depend on compensation through adaptive methylation.

Aspartate inhibition of receptor-coupled CheA activity

To examine the role of the Trp-192 residue in transmembrane signaling in more detail, we compared aspartate inhibition of the CheA kinase activity *in vitro* stimulated by the wildtype and W192A Tar receptors. We used the multisite Hill equation to draw a best-fit curve to the data (Figure 2.1), as previously described (*25*). The wild-type Tar-CheA-CheW complex had a K_i for aspartate of 7 ± 1 μM. Complexes containing W192A

Table 2.2: CheA kinase-stimulating activity of Trp-to-Ala Tar proteins[a].

Receptor	pmol CheY-P produced
None	0.24 ± 0.02
WT	44.37 ± 1.26
W192A	44.55 ± 5.80
W209A	0.26 ± 0.02
WAWA	0.48 ± 0.07

[a] CheA kinase activity was measured as described in Materials and Methods. Activities were calculated by averaging the values obtained for at least three independent membrane preparations assayed in duplicate. The error bars represent the standard deviation of the mean for these measurements.

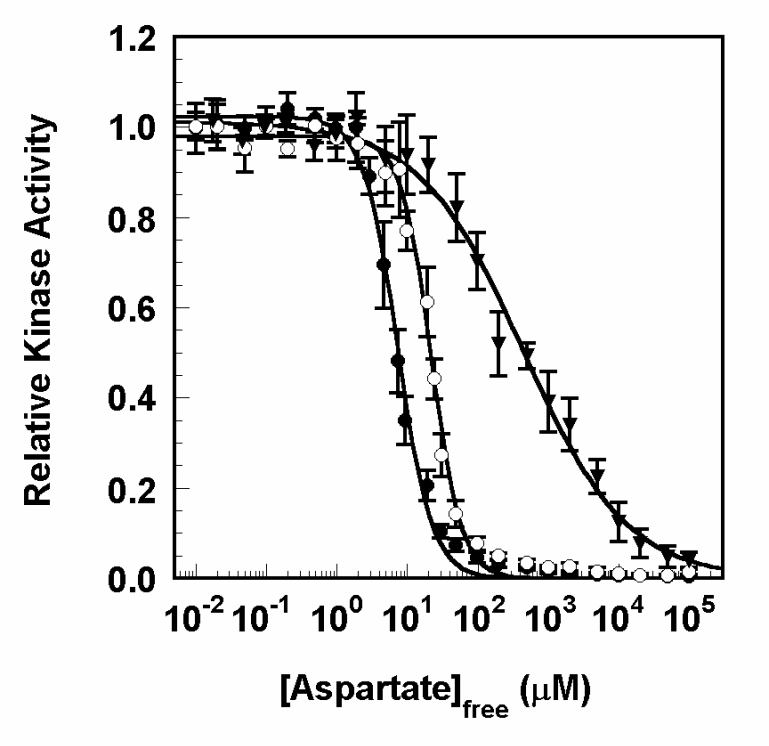

Figure 2.1. Aspartate inhibition of receptor-coupled CheA activity for W192A Tar and W211 Tar. These data are shown as closed, open circles, and closed triangles, respectively. The inhibition assays were performed as described in the Materials and Methods. Each data point represents the mean of at least six total reactions from at least three independently isolated receptor-containing vesicle preparations. The best-fit curve (solid line) is based on the cooperative multisite Hill model (*25*). The error bars represent the standard deviation of the mean when $n \geq 3$.

had a 3-fold increase in K_i to 22 ± 1 μM. The mutation did not appear to alter the cooperativity involved in aspartate-induced inhibition of CheA kinase activity, with the Hill coefficients being 1.8 ± 0.1 to 2.0 ± 0.2 for the wild-type and W192A proteins, respectively.

Effect of Trp substitutions on in vivo *methylation of Tar*

All of the Trp-substituted Tar proteins supported chemotactic swarming in aspartate and maltose semisolid agar to a significant degree. In view of the very low activity of the W209A and WAWA proteins in the *in vitro* CheA-stimulation assay, we decided to test whether compensating changes in receptor methylation restored chemotaxis. We expressed V5-tagged wild-type and mutant Tar proteins in the ΔT strain VB13 and monitored the level of Tar methylation in the absence and presence of various chemoeffectors. To provide a scale for comparing the levels of methylation, we transformed strain RP3098 with derivatives of plasmid pRD300 that produce V5-tagged Tar proteins in which the methylation sites are all Gln (QQQQ), all Glu (EEEE), or in the unmodified (QEQE) form. During SDS-PAGE, the QQQQ receptor should migrate fastest, like the fully methylated Tar protein, the unmethylated EEEE receptor should run slowest, and the QEQE receptor should migrate to an intermediate position (Figure 2.2).

With wild-type Tar proteins produced in VB13 cells, we observed two distinct bands that correspond to unmethylated and singly methylated species. Addition of a saturating concentration of aspartate (100 mM) led to a substantial increase in

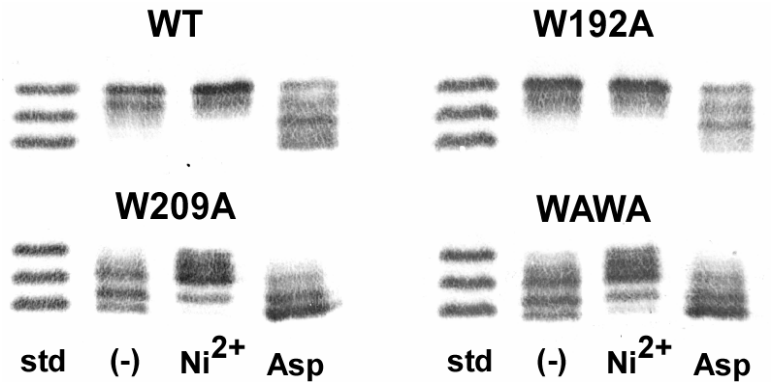

Figure 2.2. Extent of methylation of the Trp-to-Ala Tar proteins. Wild-type and mutant Tar receptors were expressed in VB13 (ΔT) cells that were exposed to aspartate and Ni^{2+}. Migration rate is affected by the level of methylation, with the more highly methylated forms moving faster. As migration standards, the EEEE, QEQE and QQQQ forms of Tar were loaded on the leftmost lane. The QEQE and QQQQ forms of Tar migrate like doubly methylated and quadrupally methylated Tar. Chemoeffectors were added to the cells as 10 mM $NiSO_4$ (repellent) and 100 mM aspartate (attractant). Equal amounts of total protein were loaded on each lane.

methylation, whereas a saturating amount (10 mM) of the repellent $NiSO_4$ caused a slight decrease. The methylation patterns of Tar W192A were nearly identical to those of the wild type.

The Tar W209A or Tar W192A W209A receptors expressed in strain VB13 showed a dramatic increase in basal methylation. This result could explain why these proteins, which fail to stimulate CheA kinase activity *in vitro* when they are in the QEQE form, support chemotactic swarming. Apparently, methylation can compensate for the low CheA stimulating activity of a receptor that lacks the cytoplasmic interfacial anchor for TM2, just as it restores activity to attractant-bound wild-type receptor.

Addition of 100 mM aspartate produced a further increase in methylation of the W209A and WAWA receptors, which exhibited higher levels of methylation than the aspartate-adapted wild-type and W192A receptors. Similarly, Ni^{2+} at 10 mM decreased methylation below the baseline level for the W209A and WAWA proteins, but the methylation was greater than for nickel-adapted wild-type or W192A Tar. Thus, adaptive methylation and demethylation occur in the absence of Trp-209, but with the absolute extent of methylation shifted to a level higher than that of wild-type Tar in naive, attractant-adapted and repellent-adapted cells.

Repositioning the cytoplasmic interfacial Trp residue alters chemotactic behavior

Since replacement of Trp-209 with Ala shifted Tar signaling in a similar manner as binding of an attractant ligand, we wondered whether the output of Tar could be more subtly modulated by moving this Trp residue in one-residue increments in the N-

terminal and C-terminal directions. We began with the Tar W209A protein and introduced Trp at each position within one helical turn of position 209. These mutants were named W206 through Tar W212 according to the position at which Trp replaced the original residue. W209 is the wild-type receptor.

We expressed these proteins in strain VB13 and analyzed their behavior in aspartate, maltose, and glycerol semisolid agar plates (Table 2.3). Three swarm phenotypes were observed. The first, seen with the W207 and W211 strains, was like wild type on all three plates. Cells expressing Tar W206 and Tar W210 formed swarms on aspartate plates like those of cells expressing Tar W209A, with very narrow, sharp chemotactic rings and rates of migration approximately half those of cells expressing wild-type Tar. Finally, cells expressing the W208 and W212 proteins failed to produce significant swarms on any of the three plates, looking just like VB13 cells containing the vector plasmid without a *tar* gene.

In vitro *stimulation of CheA activity by receptors with repositioned Trp residues*

We next analyzed the ability of the W206 through W212 receptors to stimulate CheA *in vitro* (Table 2.4). Only W209 (wild type) and W211 Tar stimulated CheA activity. Complexes containing Tar W211 produced 40 ± 7 pmol of CheY-P in 20 s and were not significantly different from wild-type Tar. We then examined the ability of aspartate to inhibit stimulation of CheA kinase by W211 Tar (Figure 2.1). The K_i value determined was 430 ± 50 μM, about 60-fold higher than the wild-type value of 7.0 ± 1

Table 2.3: Swarm behavior of cells harboring the Trp-repositioned Tar proteins [a].

Receptor[b]	Aspartate Swarm Rate	Maltose Swarm Rate	Glycerol Swarm Rate
W206	0.88 ± 0.12	0.71 ± 0.13	0.42 ± 0.04
W207	1.50 ± 0.04	0.71 ± 0.06	0.50 ± 0.04
W208	0.31 ± 0.04	0.29 ± 0.04	0.33 ± 0.01
W209 (WT)	1.72 ± 0.14	0.87 ± 0.04	0.55 ± 0.04
W210	1.03 ± 0.08	0.77 ± 0.05	0.39 ± 0.01
W211	1.81 ± 0.14	0.78 ± 0.02	0.38 ± 0.00
W212	0.09 ± 0.04	0.18 ± 0.03	0.12 ± 0.01

[a] The rate at which the swarm diameter expanded was measured in mm/hr as described in Materials and Methods.

[b] The mutant receptors Tar W206 through Tar W212 were named according to the position at which the original residue in the Tar W209A protein was replaced by Trp. This manipulation placed a single Trp residue near the cytoplasmic end of TM2 at the specified position in each mutant receptor.

Table 2.4: Effect of repositioning of Trp-209 on CheA kinase activity[a].

Receptor[b]	pmol CheY-P Produced
W206	0.42 ± 0.04
W207	0.61 ± 0.04
W208	0.80 ± 0.06
W209 (WT)	44.37 ± 1.26
W210	0.21 ± 0.02
W211	40.01 ± 7.07
W212	0.67 ± 0.11

[a] CheA kinase activity was measured as described in Table 2.

[b] The W206 through W212 receptors are described in the footnote to Table 3.

μM. The calculated Hill coefficient dropped to 0.6 ± 0.1 from the wild-type value of 1.8 ± 0.1.

In vivo *methylation of receptors with repositioned Trp residues*

To determine whether methylation compensates for the signaling biases introduced by the repositioned Trp residues, we analyzed the level of methylation of the mutant receptors (Figure 2.3). Tar W211 showed wild-type levels of methylation in the absence of chemoeffectors and after adaptation to saturating concentrations of aspartate and Ni^{2+}. The W206, W207, and W210 receptors produced methylation patterns very similar to those of the W209A and WAWA proteins. The differences in the swarm phenotypes of cells expressing W206 versus W207 Tar could be due to the greater severity of the signaling bias of the former, since the methylation levels of W207 Tar were intermediate between the wild-type and W206 proteins, and closer to the former. Tar containing Trp-208 or Trp-212 exhibited extreme overmethylation in the absence of chemoeffectors, yet these proteins partially demethylated after the addition of Ni^{2+}. Thus, even these extremely CCW-biased mutants are not totally blind to repellent stimuli, and therefore the W208 and W212 receptors cannot be "locked" in one conformation. It remains to be seen whether they can mediate a CW (tumbly) response to nickel.

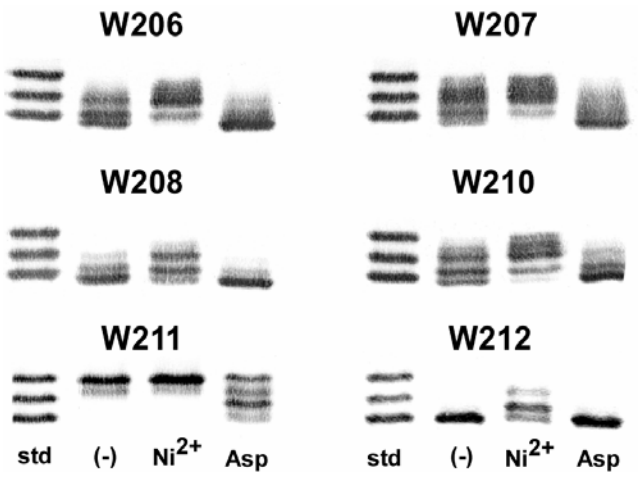

Figure 2.3. Extent of methylation of the Trp-repositioned Tar proteins. Wild-type and mutant Tar protein were expressed in VB13 (ΔT) cells and exposed to aspartate or Ni^{2+}. Analysis was as in the legend to Figure 2.3.

Motility patterns of cells expressing mutant Tar receptors

Our prediction was that compensatory methylation enables mutant cells to achieve a baseline run-tumble swimming pattern that is compatible with chemotaxis in every case except for strains expressing the W208 or W212 Tar protein. To confirm, we observed the swimming behavior of all strains using phase contrast microscopy. Strain VB13 harboring the vector plasmid pBR322 (*96*) or pRD200 carrying a *tar* gene encoding the W208 or W212 protein appeared to be almost entirely smooth swimming (Table 2.5), whereas VB13 cells carrying any other of the mutant *tar* genes tumbled with about the same frequency as cells containing the *tar*+ control plasmid.

To measure the rotational biases of the flagellar motors of the various mutants directly, we examined tethered cells (Table 2.5). As expected, VB13 cells containing the vector plasmid never reversed. The same was true for cells expressing the W212 Tar protein, and of 45 cells expressing W208 Tar, only two reversed. In contrast, the fraction of reversing cells for the other mutants was similar to the fraction of VB13 cells expressing wild-type Tar that reversed.

Discussion

A fundamental question in biolozgy is how transmembrane receptors communicate the detection of environmental stimuli to the interior of the cell. Tar, the aspartate receptor of *E. coli*, signals in response to several types of ligands by regulating the activity of its cognate histidine kinase, CheA (*15*). Disulfide-scanning experiments using Tar proteins with Cys substitutions in the first and second transmembrane helices

Table 2.5: Motile behavior of cells expressing the mutant Tar proteins

Receptor[a]	Swimming cells[b]	Tethered cells[c]		
		Cells with flagella that rotate only CCW	Cells with CCW-biased flagella that occasionally reverse	Cells with flagella that reverse frequently or show extended CCW and CW rotation
Wild type	R, s, T	5	2	23
None	S	33	0	0
W192A	R, S, t	12	2	24
W209A	R, s, T	5	0	28
WAWA	R, s, T	9	1	20
W206	R, S, T	4	1	27
W207	R, S, t	4	2	23
W208	r, S	45	0	2
W210	R, s, T	14	3	18
W211	R, S, T	6	5	25
W212	r, S	41	0	0

[a] Tar proteins are designated using the nomenclature described in the test and in footnote [b] of Table 3. None indicates that vector plasmid without a *tar* gene insert was present.

[b] Ten fields of cells swimming in TB medium at room temperature were observed for about 30 sec each. R, S, and T represent cells that were running and tumbling, smooth swimming, and primarily tumbling, respectively. Upper case letters indicate that a large fraction of the cells observed behaved in the manner indicated. Lower case letters indicate that only a few cells exhibited the behavior indicated.

[c] Tethered cells were prepared from each strain and analyzed as described in Materials and Methods.

(TM1 and TM2) of Tar strongly suggest that, upon binding of ligands, TM2 moves relative to TM1 and also to the plane of membrane (*38-44*). Here, we have examined how interactions between TM2 of Tar and the phospholipid environment influence the signaling behavior of the receptor.

We focused on the effect of Trp residues that are predicted to localize to the region between the polar headgroups and hydrophobic core of the bilayer. Glycosylation-mapping experiments (*80*) have been used to estimate the position of a transmembrane helix in the dimension perpendicular to the plane of the membrane. Such studies have shown that Trp residues exert a restoring force that can reposition synthetic helices either up or down relative to the membrane surface (*63*).

We first substituted Ala for Trp-192 and Trp-209, singly and in combination. We chose Ala as the replacement residue because we wanted to avoid introducing a residue with marked chemical properties of its own, such as charge, polarity, a high hydrophobicity index, or a reactive moiety on the side chain. The W192A protein behaved very much like wild-type Tar in every assay used, with the only consistent difference being a 3-fold increase in the K_i, from 7 μM to 22 μM, in the receptor-coupled CheA kinase assay (Figure 2.1).

In contrast, the W209A substitution drastically affected the behavior of Tar, decreasing the rate of chemotactic ring migration and eliminating receptor-mediated stimulation of CheA kinase. The WAWA double mutant behaved much like W209A, although chemotactic ring migration was slightly less impaired with the double mutant.

The combination of retained chemotactic ability coupled with lack of CheA stimulation *in vitro* associated with W209A or WAWA Tar can be explained by the compensatory role of adaptive methylation *in vivo*. Both proteins showed increased basal levels of methylation but still responded to addition of saturating aspartate (100 mM) and Ni^{2+} (10 mM $NiSO_4$) by increasing and decreasing, respectively, methylation from the altered basal level. Thus, both proteins behave in the absence of ligands as though they had undergone covalent methylation in response to attractant, but they could still mediate qualitatively appropriate responses to attractants and repellents. The tight rings formed by these mutants on aspartate swarm plates could result from a decreased dynamic range of adaptation that traps cells in the steepest portion of the gradient.

The phenotypes of the Trp-substituted mutants can be interpreted as a change in the position of TM2 relative to the membrane, thereby causing a shift in the equilibrium signaling state of the receptor. In the absence of ligand, by default Tar is in the "on" state, which stimulates the CheA kinase. Upon binding of aspartate, TM2 is predicted to slide in an axial fashion toward the cytoplasm to generate the "off" state, in which kinase activity is inhibited. We believe removal of Trp-209, with its affinity for the interfacial region, causes a slight shift of TM2 toward the cytoplasm. We speculate that the most energetically favorable repositioning upon removal of Trp-209 would be a displacement of TM2 similar to when attractant-bound receptor adopts the "off" state. Both of the proposed models for signal transmission through the HAMP linker domain (*60, 97*) involve tight regulation of the interactions between the HAMP domain and the inner membrane. This linkage could be perturbed by removal of Trp-209.

Using the same reasoning, we predict that the W192A mutation could cause a small shift in the position of the N-terminus of TM2 toward the periplasm, perhaps consistent with the 3-fold increase in the aspartate K_i of the Trp-192 receptor compared with wild type. However, the wild-type level of stimulation of CheA activity and the very slight decrease in basal methylation suggest that no significant changes are imposed on the cytoplasmic domain. Initially, this result may seem contradictory with the changes associated with the W192R mutant receptor (*42*), but the difference presumably lies with the nature of the residue that replaces Trp. Arg would be expected to interact with the negatively charged phospholipid headgroups and thus contribute a specific transmembrane-repositioning effect of its own (*98*). Thus, the W192R substitution may overcome the positioning determinants on the cytoplasmic end of TM2 and cause Tar W192R to stimulate CheA kinase more than the wild-type receptor, in contrast to our observation of a minimal difference between W192A and the wild-type receptor.

To examine how the repositioning of Trp residues within TM2 affects the signaling state of Tar, we moved Trp-209 while leaving Trp-192 in place. If Trp-209 is a primary contributor to the position of TM2 within the membrane, the signaling state of the receptor should be altered when Trp residues are scanned from positions 206 to 212 (Figure 2.4). Trp residues repositioned toward the periplasm (Trp-206 through Trp-208) should displace TM2 toward the cytoplasm and favor the "off" state (Figure 2.4B). Trp residues repositioned toward the cytoplasm Trp-210 through Trp-212 should displace TM2 farther into the membrane and favor the "on" state (Figure 2.4C).

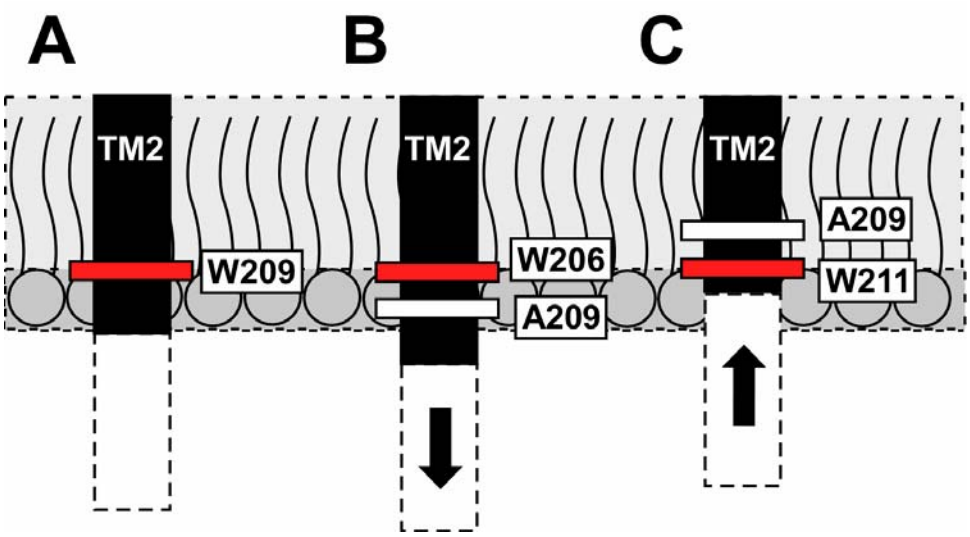

Figure 2.4. Model for the role of cytoplasmic interfacial Trp residue. TM2 is represented by a dark rectangle. Trp-209 is shown as a gray box, and the white boxes represent Ala replacing Trp. In the wild-type receptor, Trp-209 is predicted to reside within the cytoplasmic interfacial region (*42*). Upon repositioning the cytoplasmic interfacial Trp residue into the hydrophobic core, we predict a displacement of TM2 toward the cytoplasm, as represented by the downward-directed arrow. Upon repositioning a Trp residue toward the cytoplasm, we predict a displacement of TM2 into the membrane, as indicated by the upward-directed arrow.repellents boost CheA activity in the in vitro receptor-coupled assay. (Ni^{2+} at concentrations that cause a repellent response inhibits CheA activity.)

Three of the mutant proteins fulfilled the predictions of our model. W206 and W207 supported reduced but significant chemotaxis in swarm plates (Table 2.3), failed to stimulate CheA *in vitro* (Table 2.4), and showed increased basal levels of methylation (Figure 2.3). W211 formed wild-type chemotactic swarms, had a modestly increased stimulation of CheA *in vitro*, and showed normal levels of methylation *in vivo*. However, the K_i for aspartate in the *in vitro* assay increased 60-fold (7 to 430 *i*M) relative to wild-type Tar (Figure 2.1), and the Hill coefficient dropped from 1.8 to 0.6, indicating that some level of negative cooperativity might operate with the W211 protein. We do not know whether the increased K_i value reflects a lower affinity for aspartate, a partial decoupling of ligand binding and receptor inhibition, or some combination of effects. It is, however, consistent with the notion that moving the Trp residue to a more C-terminal site puts the mutant protein into a signaling conformation that is less subject to inhibition by attractant.

W211 Tar stimulated CheA activity essentially like wild-type Tar. Our prediction that the cytoplasmic end of TM2 should be pulled up into the membrane to mimic repellent-bound receptor had suggested to us that the W211 protein might support a higher rate of CheA autophosphorylation. We note however, that no one has shown that Tar repellents boost CheA activity in the *in vitro* receptor-coupled assay. (Ni^{2+} at concentrations that cause a repellent response inhibits CheA activity.)

Cells expressing the W208 and W212 proteins are completely nonchemotactic (Table 2.3). Their lack of receptor-coupled CheA activity *in vitro* is shared with the W206, W207, and W210 proteins (Table 2.4), but the first two receptors differ from the

latter three in that those proteins are restored to some level of function *in vivo* by adaptive methylation. The W208 and W212 proteins are stable when overexpressed (data not shown) and are also present at normal levels *in vivo* (Figure 2.3), where they are very highly methylated. In fact, W212 exists solely in the highest methylated form. However, these proteins are not totally inert, since addition of aspartate further increases methylation of the W208 protein, and Ni^{2+} leads to demethylation of both proteins. The W208 and W212 proteins cannot support chemotaxis because their signaling bias is set so far toward CCW that the cells rarely, if ever, tumble (Table 2.5).

One explanation for the grossly disrupted function of the W208 and W212 receptors is suggested by a helical-wheel projection of TM1 and TM2 of the receptor homodimer (*38*). The side chains of residues Ala-208 and Ile-212 are directed toward TM2 and TM1 of the other subunit, respectively. Insertion of a bulky Trp residue at either of these positions may disrupt the helical packing face, as has been seen in the transmembrane proton channel of the MotAB complex (*99*, *100*) or the dimer-dimer interface in the trimer of dimers in the cytoplasmic domain of the Tsr receptor (*68*). However, other interpretations are equally plausible.

Perhaps the most informative Trp mutant is the double mutant W209A/Y210W. The W210 protein generated by these two substitutions behaves much like W209A. We attribute the signaling abnormalities of the latter protein to the loss of Trp-209. The residue that Trp replaces at position 210 is Tyr. Thus, both the wild-type and W211 proteins have tandem amphipathic aromatic residues (either WYG or AYW at positions 209-211), whereas the W210 and W209A proteins have a single aromatic residue (AWG

or AYG, respectively). Preliminary data (Draheim, *unpublished*) suggest that juxtaposed aromatic residues are required for proper positioning of the cytoplasmic end of TM2.

Bacterial chemoreceptors resemble many members of a large family of homodimeric transmembrane sensor kinases (*68*). Functional chimeras have been made that join the periplasmic, transmembrane, and linker domains of Tar (*101*) and Trg (*102*) to the signaling domain of the sensor kinase EnvZ. In a reciprocal chimera, the periplasmic, transmembrane, and linker domains of the NarX kinase were connected to the signaling and adaptation domains of Tar to create a nitrate/nitrite repellent receptor (*103*). An alignment of the C-terminal portion of TM2 from the four *E. coli* chemoreceptors and all *E. coli* transmembrane sensor kinases with P-type linker domains (Figure 2.5) reveals that most have one or more aromatic residues closely preceding the highly conserved Pro residue that begins the linker. The function of these aromatic residues, particularly Trp and Tyr, may be to orient the receptor with respect to cytoplasmic face of the cell membrane. Both EnvZ and NarX possess a Trp residue at the cytoplasmic end of TM2.

Our results provide additional evidence of the importance of interactions between TM2 and the surrounding phospholipid environment and demonstrate the crucial role of the Trp residue at the C-terminus of TM2. Such considerations will be important for the design of chemoreceptors and other transmembrane sensors with specific functions. It also appears that tandem aromatic residues may be required for optimal localization of TM2 with respect to the cytoplasmic face of the cell membrane, a possibility that is currently under investigation.

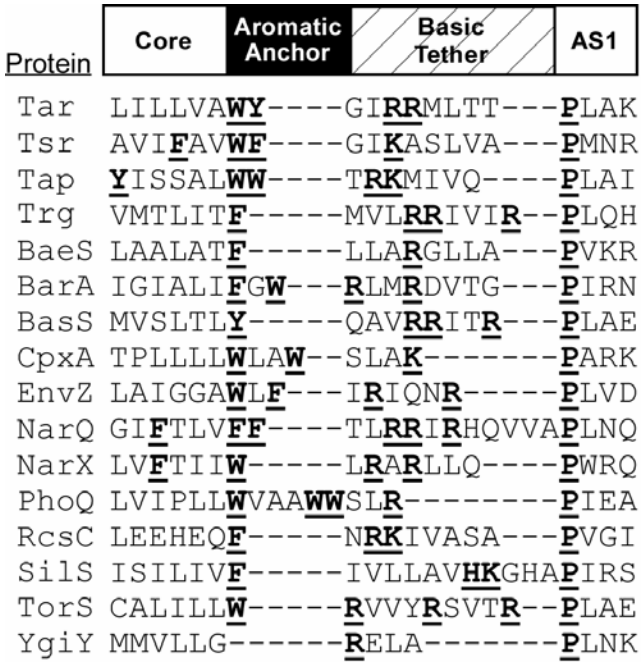

Figure 2.5. Sequence alignment of the C-termini of TM2 from membrane-spanning receptors in *E. coli*. All proteins predicted to contain only two TM helices and a P-type linker (*60*) are shown. The conserved Pro residue at the N-terminus of the first amphipathic helix (ASI) of the linker region provided the reference point for the alignment. An evident shared motif consists of one or more aromatic residues that may serve as an anchor within the interfacial zone of the membrane and a basic tether that should interact strongly with negatively charged polar head groups. The sensor kinases mediate responses to environmental conditions: stress on the cell envelope (BaeS, CpxA, SliS); expression of virulence genes (BarA, PhoQ); biofilm formation (RcsC); environmental osmolarity (EnvZ); use of alternative electron acceptors nitrate/nitrite (NarQ, NarX) and TMAO (TorS); or of unknown function (BasS, YgiY).

CHAPTER III

TUNING A BACTERIAL CHEMORECEPTOR WITH PROTEIN-MEMBRANE INTERACTIONS*

Overview

This chapter is a published work (*44*). It describes research that manipulates protein-membrane interactions between the second transmembrane domain (TM2) and the cell membrane to incrementally modulate the basal signaling state of Tar. I conceived and conducted the majority of the experimentation described within this chapter. Dr. Arjan F. Bormans established the protocol for determining the extent of methylation *in vivo* and performed some of the experiments described in Figure 3.5. Dr. Run-zhi Lai and I worked together to establish the protocol and purify the proteins necessary for the receptor-coupled *in vitro* phosphorylation assay used in Figure 3.6.

Summary

Chemoreceptors in *Escherichia coli* are homodimeric transmembrane proteins that convert environmental stimuli into intracellular signals controlling flagellar motion. Chemoeffectors bind to the extracellular (periplasmic) domain of the receptors, whereas their cytoplasmic domain mediates signaling and adaptation. The second transmembrane helix (TM2) connects these two domains. TM2 contains an aliphatic core flanked by

---

amphipathic aromatic residues that have specific affinity for polar-hydrophobic membrane interfaces. We previously showed that Trp-209, near the cytoplasmic end of TM2, helps maintain the normal baseline-signaling state of the aspartate chemoreceptor (Tar) and that Tyr-210 plays an auxiliary role in this control. We have now repositioned the Trp-209/Tyr-210 pair in single-residue increments about the cytoplasmic polar-hydrophobic interface. Changes from WY-2 to WY+1 modulate the baseline signaling state of the receptor in predictable and incremental steps that can be compensated by adaptive methylation/demethylation. Greater displacements, as in WY-3, WY+2, and WY+3, bias the receptor to the "off" kinase-inhibiting state or the "on" kinase-stimulating state, respectively, to a degree that cannot be fully compensated by the adaptation system. Aromatic residues analogous to Trp-209/Tyr-210 are present in other chemoreceptors and many transmembrane sensor kinases, where they may serve a similar function.

Introduction

Escherichia coli cells migrate in chemical gradients using a behavior known as chemotaxis. In a homogeneous environment, cells perform a three-dimensional random walk in which smooth swims (runs) of several seconds alternate with briefer periods of active, random reorientation (tumbles). Movement in the gradient is accomplished by selectively increasing the length of runs that happen to lead in a favorable direction, whether up an attractant gradient or down a repellent gradient (*12-14*). The signal-transduction pathway modulates flagellar motion to increase intervals of exclusively counter-clockwise (CCW) rotation, which produces runs, when the bacterium senses an

increase in attractant or a decrease in repellent over time. Thus, a spatial gradient is sensed by temporal comparison of chemoeffector concentrations.

The histidine protein kinase CheA is coupled, via the CheW adapter protein, to four different methyl-accepting chemotaxis proteins, known as MCPs (*104*), and to the Aer redox sensor (*3, 4*). A receptor/CheA/CheW ternary complex (*105*) stimulates CheA autophosphorylation (*15*). The phosphoryl group on CheA is then transferred to the response regulator CheY. Phospho-CheY interacts with FliM of the flagellar motor to promote clockwise (CW) rotation (*17, 18*).

CCW motor rotation coalesces the left-handed helical flagellar filaments into a bundle that propels the cell in a run (*10*), whereas CW rotation of one or more flagella disrupts the bundle to cause a tumble (*11*). The intracellular level of phospho-CheY, and hence the frequency of tumbling, is determined by the relative activities of CheA and the phospho-CheY phosphatase, CheZ (*16, 19*). The conformational change induced by attractant binding converts a receptor from a stimulator (50-100× increase) of CheA activity into an inhibitor (5× decrease) of CheA (*15*). The resulting drop in the intracellular phospho-CheY level lowers the probability of tumbling and thereby lengthens the average run.

Inhibition of CheA activity is balanced by covalent methylation of the cognate receptor (*21*). Methyl groups are added by a methyltransferase, CheR, and removed by CheB, a methylesterase (*22, 23*). CheB is active when phosphorylated by CheA (*24*). Increased methylation of four specific Glu residues biases a receptor toward CheA stimulation, whereas decreased methylation results in less CheA stimulation (*25, 26*). By

constantly adjusting the extent of methylation, a cell can maintain nearly the same baseline level of CheA activity at any constant concentration of chemoeffector (*27*), and adaptation is robust (*106*).

Tar is the aspartate/maltose chemoreceptor in *E. coli* (*32*). The crystal structure of the periplasmic ligand-binding domains of *Salmonella* (*35, 46*) and *E. coli* (*47*) Tar show that each monomeric unit of the functional homodimer (*48, 49*) consists of four anti-parallel α-helices in a four-helix bundle. The first and second transmembrane regions (TM1 and TM2) flanking the periplasmic domain are N-terminal and C-terminal, respectively, helical extensions of the first (H1) and fourth (H4) periplasmic helices (*50-53*). Aspartate binds at one of two rotationally symmetric sites composed of residues in H1 and H4 of one monomer and in H1' of the other (*46*). Binding generates a 1 to 2 ångström vertical displacement of H4-TM2 toward the cytoplasm (*38-44*). Within the HAMP-linker domain (*59-61*), this piston-like movement is converted into a conformational change in the cytoplasmic domain of the receptor.

TM2 possesses an aliphatic core bracketed by aromatic residues at the polar-hydrophobic interfaces, and positively charged residues reside at the membrane-water interface (*42*). A similar distribution of hydrophobicity, aromaticity, and charge density is often found in membrane-spanning α helices (*79*). Several experimental systems have demonstrated the energetic advantage for the localization of amphipathic aromatic residues at the polar-hydrophobic interfaces. A glycosylation-mapping technique (*80*) implicated Trp residues in positioning a poly-Leu helix within a biological membrane. When the Trp residues were moved, the helix repositioned to allow the Trp residues to

remain at the interfacial zone of the membrane (*63*). Also, WALP (*81*) and YALP (*107*) peptides consisting of Ala-Leu cores of different lengths flanked by Trp or Tyr residues, respectively, induce phase transitions in various lipid systems that allow the aromatic residues to reside at polar-hydrophobic interfaces. Thus, amphipathic aromatic residues govern how transmembrane helices interact with their lipid environments.

The position of TM2 relative to the membrane is a critical component of transmembrane signaling. Therefore, interactions between TM2 and the phospholipid bilayer are likely to contribute to the baseline-signaling state of a receptor. Arginine-scanning mutagenesis of *Salmonella* Tar revealed the importance of aromatic residues within TM2. Substitution of Phe-189 or Trp-192 stabilized the kinase-stimulating "on"-state of Tar, while substitution of Trp-209 promoted the kinase-inhibiting "off"-state (*42*). We previously demonstrated that Trp-209 is essential for maintaining the normal baseline-signaling state of *E. coli* Tar. Substitution of Ala for Trp-209 puts the mutant receptor into the kinase-inhibiting state typically associated with binding of aspartate. Tyr-210 also contributes to positioning of TM2 within the lipid bilayer (*43*). These prior studies identified residues participating in essential membrane-protein interactions that position TM2 within the membrane. Here, we extend these initial analyses by moving the Trp-209/Tyr-210 pair in single-residue increments three positions toward the N-terminus (WY-3) and three positions toward the C-terminus (WY+3). We demonstrate that, within the context of an intact chemotactic circuit, moving the Trp/Tyr pair "tunes" the signaling state of Tar in predictable and incremental steps.

Materials and methods

Bacterial strains and plasmids

Strains HCB436 [Δ*tsr7021 Δtrg(100) zbd::Tn5* Δ(*tar-cheB)2234*] (*108*), RP3098 [Δ*(flhD-flhB)4*] (*85*) and VB13 [Δ*tsr7021* Δ*tar-tap5201 trg*::Tn*10*] (*86*) are derivates of the *E. coli* K12 strain RP437 (*85*). Plasmid pRD100 (*43*), derived from pBAD18 (*88*), carries a wild-type copy of *tar* inducible upon addition of L-arabinose. Plasmid pRD200 (*43*), derived from pMK113 (*87*), harbors a version of the *tar* gene that encodes wild-type Tar attached to a C-terminal in-frame sequence for a seven-residue flexible linker and a V5-epitope tag. The *tar* gene of pRD200 is expressed from the native *tar* promoter. Plasmid pRD300 is identical to pRD100 except for the addition of the C-terminal linker and V5-epitope tag from pRD200. Mutations were introduced into *tar* using standard site-directed mutagenesis techniques (Stratagene).

Observation of tethered cells

Cells were grown in tryptone broth (*91*) supplemented with 25 μg/mL ampicillin to an OD_{590nm} of 0.7. Ten mL of cells were resuspended in tethering buffer [10 mM potassium phosphate (pH 7.0), 100 mM NaCl, 10 μM EDTA, 20 μM L-methionine, 20 mM sodium DL-lactate, 20 μg/ml chloramphenicol], and their flagella were sheared in the 50-mL stainless-steel cup of a Waring blender (*109*). Sheared cells were washed twice in tethering buffer and mixed with an equal volume of a 500-fold dilution of anti-flagellar filament antibody. This mixture was placed inside an Apiezon-L grease ring on a 12 mm round coverslip, incubated for 30 min at 30ºC, and then affixed to a flow

chamber (*92*). Tethered cells were observed at 1000x magnification by oil-immersion, reverse-phase contrast microscopy. Enough fields of view were videotaped to ensure that at least 100 freely rotating cells were monitored for each strain in two duplicate experiments. Rotational behavior was visually assessed during video playback, and cells were assigned to one of five rotational categories; exclusively CCW; mostly CCW with occasional reversals; reversing frequently with no clear bias; mostly CW with reversals; and exclusively CW. Reversal frequency was determined by tallying the number of reversals for each cell during video playback.

Determination of the methylation state of receptors in vivo

Cells were grown to an OD_{590nm} of 0.6 in 10 mL of tryptone broth (*91*), harvested by centrifugation, washed three times with 10 mM potassium phosphate (pH 7.0) containing 0.1 mM EDTA, and resuspended in 5 mL of 10 mM potassium phosphate (pH 7.0), 10 mM sodium DL-lactate, and 200 μg/mL chloramphenicol. One-mL aliquots of cells were transferred to 10-mL scintillation vials and incubated with shaking for 10 min at 32^{o}C. Cells were then incubated for another 30 min after the addition of L-methionine to 2 μM. Chemoeffectors were added at this time, and the cells were incubated for an additional 20 min. Reactions were terminated by addition of 100 μL ice-cold 100% TCA and then incubated on ice for 15 min. Denatured proteins were pelleted, subsequently washed with 1% TCA and acetone, and resuspended in 200 μL 2X SDS-loading buffer. A 10-μL aliquot of each sample was subjected to SDS-PAGE

immunoblotting and detection by commercially available antibodies raised against the V5 epitope (Invitrogen).

Protein expression and isolation

We isolated receptor-containing inner membranes as previously described (*73*). Strain RP3098 harboring pRD100 or one of its derivatives was used for production of receptor-containing membranes. Tar expression was induced by addition of L-arabinose to a final concentration of 0.2% (w/v). Soluble Che proteins were isolated as previously described (*73*).

In vitro *analysis of receptor function*

We performed the receptor-coupled *in vitro* phosphorylation assay as previously described (*43*). Our reactions contained 20 pmol Tar, 5 pmol CheA, 20 pmol CheW, and 500 pmol CheY in 9 μL of fresh phosphorylation buffer [50 mM Tris-HCl, 50 mM KCl, 5 mM $MgCl_2$, 2 mM DTT (pH 7.5)]. Aspartate was added to the desired final concentration, taking care to maintain the same total volume. The reaction was initiated by addition of 1 μL of [γ-^{32}P]-ATP (3000 Ci/mmol NEN# BLU502A) diluted 1:1 with 10 mM unlabeled ATP. Reactions were terminated by adding 40 μL 2X SDS-PAGE loading buffer containing 25 mM EDTA. Samples were subjected to SDS-PAGE, dried, and imaged using a phosphorimager (Fuji BAS 5000).

Chemotactic swarm assays

Swarm assays were performed as described previously (*43*). Briefly, semi-solid agar contained 3.25 g/L Difco BactoAgar in motility medium [10 mM potassium phosphate (pH 7.0), 1 mM $(NH_4)_2SO_4$, 1 mM $MgSO_4$, 1 mM $MgCl_2$, 1 mM glycerol, 90 mM NaCl] supplemented with 20 μg/mL of L-threonine, L-histidine, L-methionine, and L-leucine and 1 μg/mL thiamine. Ampicillin was present at 25 μg/mL. Aspartate and maltose were added to a final concentration of 100 μM. Swarm plates were incubated at 30ºC and, once visible swarms formed, their diameter was measured every 4 h.

Results

Repositioning Trp-209/Tyr-210 of TM2 relative to the polar-hydrophobic membrane interface

We have shown that Trp-209 is essential for maintaining the normal baseline-signaling state of Tar and suggested that Tyr-210 plays an auxiliary role in this control (*43*). Inspired by these results and the demonstrated affinity of amphipathic aromatic residues for the polar-hydrophobic interfaces of phospholipid bilayers (*63, 64, 79, 81, 83*), we hypothesized that the signaling state of Tar could be modulated by repositioning the tandem residue pair Trp-209/Tyr-210, which localizes to the polar-hydrophobic interface at the cytoplasmic side of the cell membrane (*42*). We used site-directed mutagenesis to construct receptors in which the Trp/Tyr pair was repositioned in single-residue increments from three residues N-terminal of their original position (WY-3) to three residues C-terminal (WY+3) (Figure 3.1).

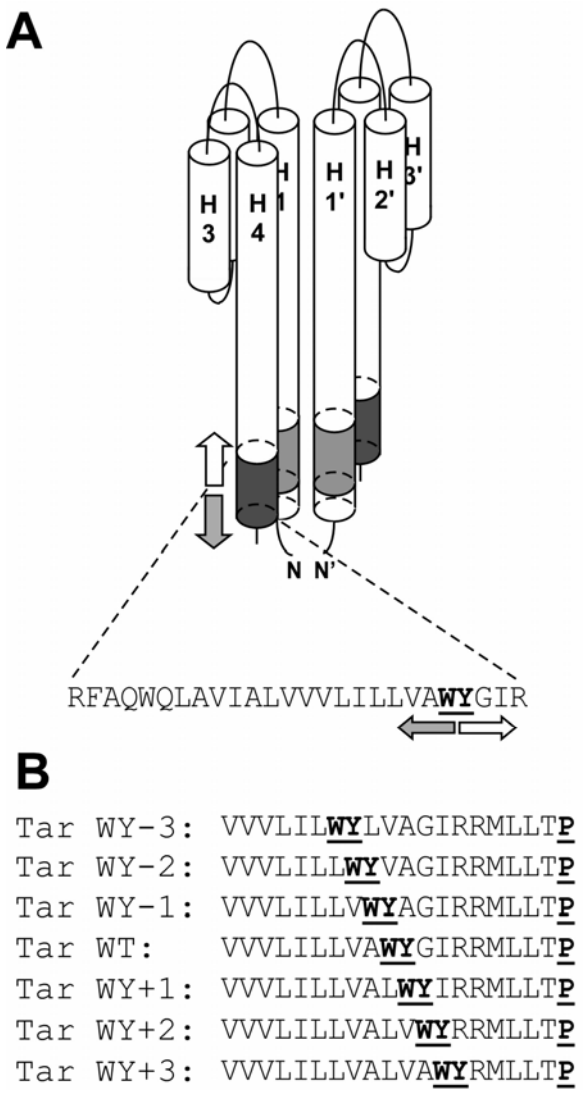

Figure 3.1. TM2 sequences of the Trp/Tyr-repositioned Tar proteins. (A) TM1 and TM2 are represented as gray- and black-shaded areas, respectively. Aspartate binding displaces TM2 toward the cytoplasm, thereby repositioning TM2 relative to the plane of the phospholipid bilayer (downward gray arrow). Repellent binding displaces TM2 away from the cytoplasm (white upward arrow). The extent of TM2 is based on sulfhydryl-reactivity studies of *S. enterica* Tar (*42*) and includes the Trp-209 and Tyr-210 residues (boldface). (B) Primary sequences of TM2 of the full range of Tar proteins investigated in this study. The Trp/Tyr residue pair is indicated in boldface. The conserved Pro residue of P-type HAMP-linker domains (*60*) provides a reference for the beginning of AS1. The gray, leftward-pointing arrow indicates shifts of the Trp/Tyr pair in the N-terminal (-) direction. The white, rightward-facing arrow indicates shifts of the Trp/Tyr pair in the C-terminal (+) direction.

Flagellar rotation and reversal frequency correlate with the position of the Trp-Tyr pair

We tested the hypothesis that repositioning Trp-209/Tyr-210 would result in a displacement of TM2 relative to the membrane and a concomitant change in the baseline-signaling state of the receptor (Figure 3.1). Rotational bias and reversal frequency in the absence of chemoeffectors were measured in transducer-depleted (ΔT) tethered cells (strain VB13; *86*) expressing the WY-3 through WY+3 Tar receptors from plasmid pRD200. Expression from pRD200 results in a five-fold excess of total cellular receptor (data not shown). These cells possess an intact chemotactic circuit, and therefore their behavior should reflect steady-state signaling, which is affected by changes in both the position of TM2 relative to the membrane and the compensatory effects of adaptive methylation (*43*). Approximately 200 cells were analyzed for each receptor variant (Figure 3.2). Most cells producing wild-type Tar reversed frequently and showed the same CW/CCW bias (between 20/80 and 40/60%) previously observed with the wild-type strain RP437. A few cells reversed less frequently and were more strongly CW or CCW biased, and a very small number of cells were observed to rotate exclusively in one direction or the other.

Flagella of cells harboring Tar WY-1 or Tar WY-2 exhibited a slight CCW rotational bias compared to those expressing wild-type Tar, and cells expressing WY-3 Tar were even more CCW biased. A CCW bias indicates that these cells had a decreased intracellular concentration of phospho-CheY (*19*), a result consistent with decreased stimulation of CheA by a receptor bearing a displacement of TM2 toward the cytoplasm (*38*). Cells expressing Tar WY+1 were very similar to cells producing the wild-type

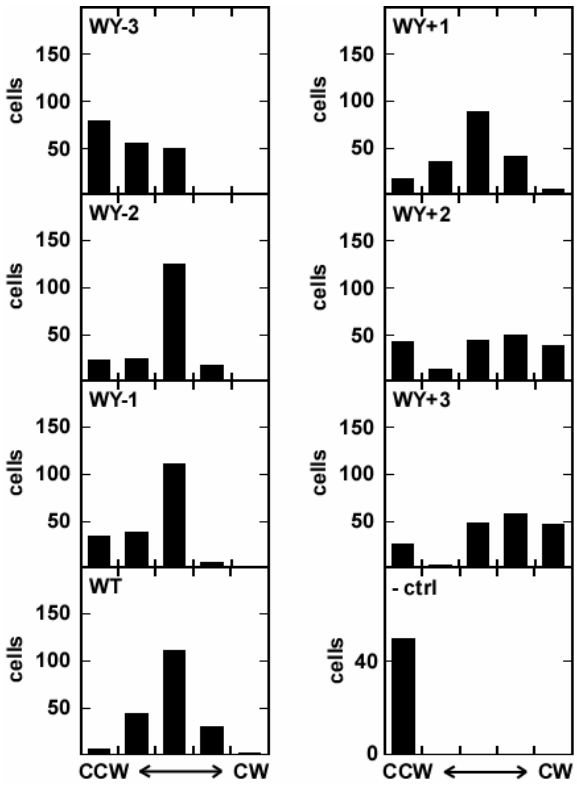

Figure 3.2. The directional bias of flagellar rotation correlates with the position of the Trp/Tyr pair. Transducer-depleted VB13 (*cheR*$^+$*B*$^+$) cells expressing the wild-type or mutant Tar proteins from plasmid pRD200 were tethered, observed for 30 s, and placed into one of five categories based on the CW/CCW rotational behavior of their flagella. The five categories of rotation, from left to right, are: exclusively CCW; mostly CCW with occasional reversals; reversing frequently with no clear bias; mostly CW with reversals; and exclusively CW. Control (ctrl) cells (bottom right) contained only the empty vector plasmid. Two sets of 100 cells were analyzed for each strain.

receptor. WY+2 and WY+3 Tar cells exhibited a bimodal distribution; the majority were CW biased, but some cells were observed whose flagella rotated exclusively CCW. A CW bias is characteristic of increased intracellular levels of phospho-CheY (*19*) and is consistent with the expectation that displacement of TM2 toward the periplasm should increase the ability of a receptor to stimulate CheA activity.

The mean reversal frequency (MRF) was approximately $0.4 \cdot sec^{-1}$ for cells expressing WY-2, WY-1, wild-type, and WY+1 Tar. Cells expressing WY-3 Tar had an MRF of $0.2 \cdot sec^{-1}$, whereas cells expressing WY+2 and WY+3 Tar had an MRF of $0.25 \cdot sec^{-1}$ (Figure 3.3). We conclude that cells expressing WY-3, WY+2, and WY+3 Tar have reduced MRF values because the signaling state of these receptors is perturbed to an extent that cannot be entirely compensated by adaptive methylation.

Cells lacking adaptive methylation cannot compensate for TM2 displacements.

To assess the contribution of adaptive methylation to the signaling state of Tar, we analyzed flagellar rotation in strain HCB436 (ΔT Δ*cheRB*) (*108*). HCB436 cells expressing wild-type Tar displayed a slight CW bias (Figure 3.4) and high MRF values ($\sim 0.55 \cdot sec^{-1}$) (Figure 3.3). HCB436 cells producing the WY-3 through WY-1 receptors seldom, if ever, rotated CW (Figure 3.4). These cells clearly had lower levels of intracellular phospho-CheY than VB13 (ΔT $cheR^{+}B^{+}$) cells expressing the equivalent mutant receptors. This finding is consistent with our previous discovery (*43*) that methylation can compensate for an inherently decreased baseline-signaling state of a receptor. The WY+1 protein conferred a modest CW bias to HCB436 cells. Cells

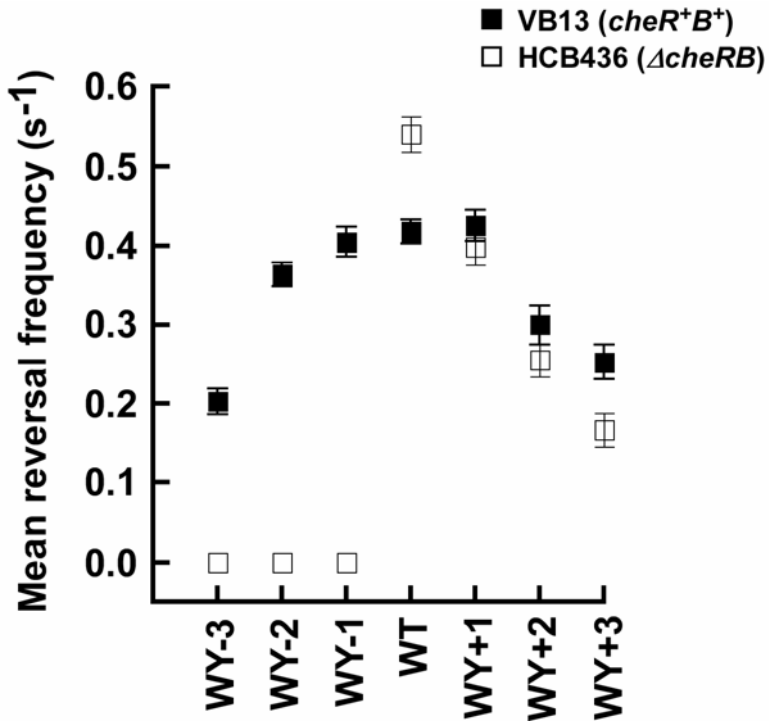

Figure 3.3. Mean reversal frequency (MRF) correlates with the position of the Trp-Tyr pair. The same 200 VB13 cells (*cheR*$^{+}$*B*$^{+}$) analyzed in Figure 3.2 (closed squares) and 200 HCB436 cells (Δ*cheRB*) (open squares) expressing each wild-type or mutant Tar protein from plasmid pRD200 were tethered as described in Figure 3.2. Cells were monitored for 30 s, and the number of reversals was determined. Each data point represents the mean number of reversals per second. The error bars represent the standard deviation of the mean, with n = 200.

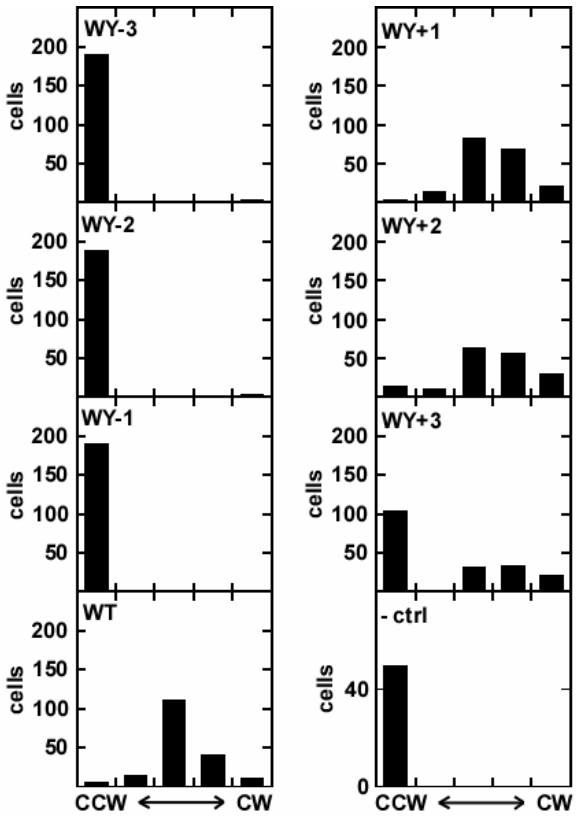

Figure 3.4. Cells deficient in methylation exhibit severe changes in flagellar rotation upon repositioning Trp-209/Tyr-210. The same 200 HCB436 cells (Δ*cheRB*) of each strain for which MRF values were determined (Figure 3.3) were analyzed as in Figure 3.2.

producing WY+2 and WY+3 were also CW biased relative to cells expressing wild-type Tar, but a significant number of cells rotated their flagella only CCW. Such cells were also seen when the WY+2 and WY+3 proteins were expressed in strain VB13 (Figure 3.2), although the fraction of CCW-only cells was lower.

Methylation of mutant receptors in vivo

To demonstrate that methylation restores a more-normal baseline-signaling state for the mutant receptors, we analyzed methylation *in vivo*. To create standards for comparison, we expressed the all Gln (QQQQ), all Glu (EEEE), and wild-type (QEQE) forms of Tar in strain RP3098 [*ΔflhD-flhB*] (*84*). During SDS-PAGE, the QQQQ form migrates fastest, the EEEE form slowest, and the QEQE form at an intermediate rate (Figure 3.5). WY-1 and WY-2 exhibited increased levels of methylation *in vivo* that were apparently adequate to compensate completely for the inherent CCW bias associated with those receptors in the absence of adaptive methylation (compare Figures 3.2 and 3.4). WY-3 Tar had equivalently elevated levels of methylation, but in this case only partial compensation for the inherent CCW bias (Figure 3.2) associated with the mutant receptor was seen.

In contrast, WY+1 Tar had a very slight decrease in its methylation level compared to wild-type Tar, a finding consistent with the wild-type rotational bias of VB13 cells containing this protein. The methylation level observed with WY+2 and WY+3 Tar was significantly decreased relative to wild-type, but the CW bias of VB13

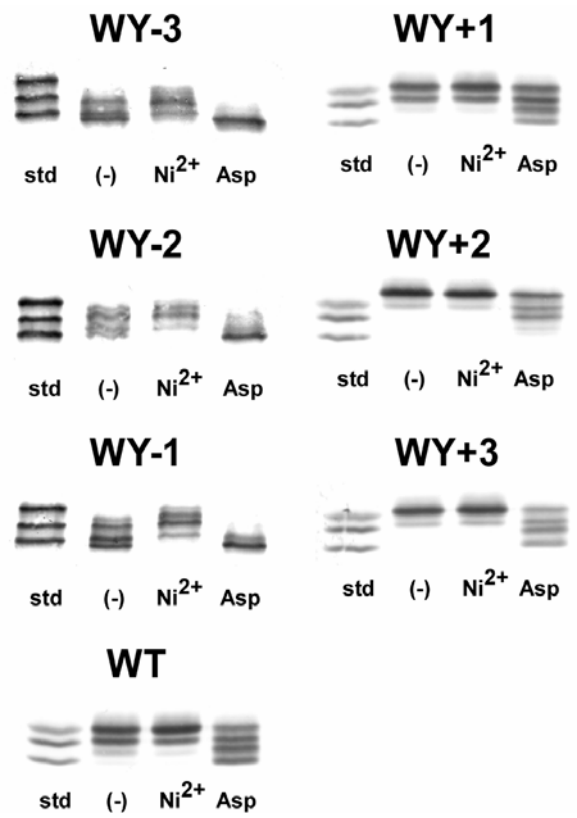

Figure 3.5. Extent of methylation of Trp/Tyr-repositioned Tar proteins. Transducer-depleted VB13 cells expressing the wild-type or mutant Tar proteins from plasmid pRD200 were exposed to 100 mM aspartate or 10 mM Ni^{2+}. The level of methylation affects the migration rate during SDS-PAGE, with the more-highly methylated forms moving faster. As migration standards, the EEEE, QEQE, and QQQQ forms of wild-type Tar were loaded in the leftmost lane. The QEQE and QQQQ forms of Tar migrate like the doubly methylated and quadruply methylated Tar, respectively.

cells expressing either of those proteins demonstrated that adaptive demethylation cannot completely offset the inherent CW bias imposed by those two receptors.

Apparently, none of the mutant receptors were locked in one conformation. The WY-3 to WY-1 receptors all showed increases in methylation in response to addition of 100 mM aspartate (Figure 3.5), although the change with the WY-3 protein was slight. Similarly, all of these receptors became less methylated after addition of 10 mM of the Tar-mediated repellent Ni^{2+} (Figure 3.5). Little change was seen in the methylation state of the wild-type or WY+1, WY+2, and WY+3 proteins in response to Ni^{2+}, but all four proteins became more substantially more methylated after addition of 100 mM aspartate.

Mutant Tar receptors possess reduced sensitivity to aspartate.

Based on the results described thus far, we proposed that the signaling state of Tar correlates with the position of the Trp-209/Tyr-210 pair at the cytoplasmic polar-hydrophobic interface. Furthermore, the mutant receptors still react to either, or both, aspartate (attractant) and Ni^{2+} (repellent) (Figure 3.5). It has been suggested that methylation of MCPs in receptor/CheA/CheW ternary complexes causes adaptation by altering the gain between ligand binding and kinase inhibition without substantially altering ligand affinity or kinase stimulation (*72*). If this is true, receptors producing wild-type rotational phenotypes (Tar WY-2 to Tar WY+1) should exhibit different sensitivities to ligand in proportion to the extent of methylation required to maintain a wild-type rotational bias.

To test this prediction, we expressed both wild-type and mutant receptors from plasmid pRD200 in VB13 (ΔT) cells and analyzed chemotactic migration in motility agar containing aspartate (Figure 3.6A), maltose, or glycerol (data not shown). Glycerol is a non-attractant carbon source that allows for analysis of aerotaxis in the absence of any specific Tar chemoeffector. Repositioning of Trp-209/Tyr-210 invariably decreased the migration rate to a degree that correlated with the distance they were moved. This was true even for cells expressing Tar WY-2, Tar WY-1, and Tar WY+1, which possess similar baseline rotational biases (Figure 3.2) and MRFs (Figure 3.3). We conclude that when Trp-209/Trp-210 are at their original positions, the receptor possesses a level of methylation that allows optimal sensitivity to a gradient of attractant. We also examined the ability of the mutant receptors to stimulate CheA in the receptor-coupled *in vitro* phosphorylation assay (*15, 43*), which is performed in the absence of CheR and CheB. We isolated the inner membranes from RP3098 cells in which Tar was expressed from plasmid pRD100. All Tar in these membranes should be in the QEQE form in which it is initially translated. Tar constituted between 40 and 60 percent of total protein in all of the membrane preparations, demonstrating that all of the mutant proteins are reasonably stable. Receptor/CheA/CheW complexes containing wild-type Tar produced 7.8 ± 1.2 pmol phospho-CheY·s^{-1} (Figure 3.6B). The WY-3 through WY-1 receptors all stimulated CheA to less than 10 percent of this value, a result consistent with displacement of TM2 toward the cytoplasm and the absence of adaptive methylation. The WY+1 to WY+3 receptors all retained the ability to stimulate CheA. The somewhat reduced activities of

Figure 3.6. Mutant receptors exhibit decreased ligand sensitivity. (A) The rate at which the swarm diameter increased, measured in mm/h, was analyzed for VB13 cells expressing wild-type or mutant receptors from plasmid pRD200. The error bars represent the standard deviation of the mean, with n = 3. (B) CheA kinase-stimulating activity was measured for membranes containing the wild-type and mutant Tar proteins. CheA activities were calculated by averaging the values obtained for at least three independent membrane preparations, each of which was assayed in triplicate. The error bars represent the standard deviation of the mean, with n = 9. All receptors were in the QEQE configuration. (C) Aspartate-inhibition of receptor-coupled kinase activity of receptor/CheA/CheW complexes containing wild-type (filled circles), WY+1 (filled squares), WY+2 (filled diamonds), and WY+3 (filled triangles) Tar proteins. Each data point represents the mean of six total reactions from three independently isolated receptor-containing vesicle preparations. The best-fit curves, represented in blue for the wild-type receptor and red for the mutants, were calculated using the cooperative Hill model. The error bars represent the standard deviation, with n = 3.

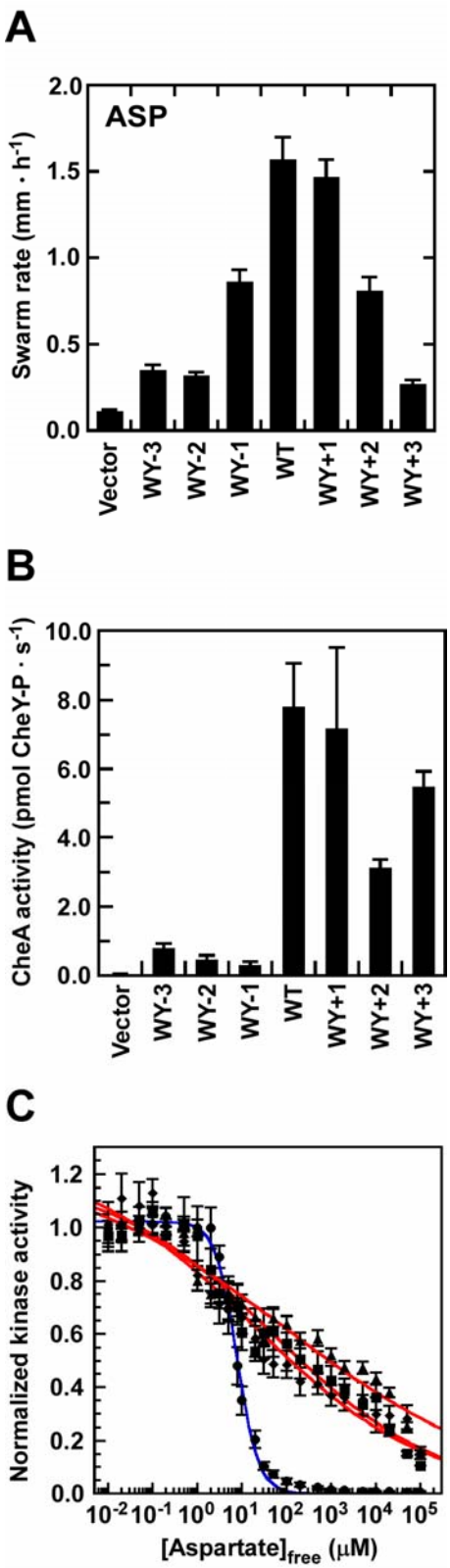
A
ASP
Swarm rate (mm · h-1)
2.0
1.5
1.0
0.5
0.0
Vector
WY-3
WY-2
WY-1
WT
WY+1
WY+2
WY+3
B
CheA activity (pmol CheY-P · s-1)
10.0
8.0
6.0
4.0
2.0
0.0
Vector
WY-3
WY-2
WY-1
WT
WY+1
WY+2
WY+3
C
Normalized kinase activity
1.2
1.0
0.8
0.6
0.4
0.2
0.0
10-2 10-1 100 101 102 103 104 105
[Aspartate]free (μM)

WY+2 and WY+3 Tar suggest that the transmembrane, HAMP-linker, and cytoplasmic domains may be "out of register," somehow resulting in decreased CheA activity.

We also examined the aspartate-induced inhibition of CheA activity for wild-type and mutant receptors *in vitro*. The multisite Hill equation was used to draw a best-fit curve to the data (Figure 3.6C). With wild-type-Tar, the aspartate K_i was 7 ± 1 μM, and the Hill coefficient was 1.8 ± 0.1, suggesting positive cooperativity. The WY+1 through WY+3 receptors had aspartate K_i values between 10 and 100 μM. Most strikingly, the Hill coefficients were in the range 0.2 ± 0.1, suggesting that there was a strong negative cooperativity for aspartate inhibition.

Methylation has been suggested to cause adaptation by altering the gain between ligand binding and kinase inhibition without altering ligand affinity or kinase stimulation (*72*). Therefore, we hypothesized that receptors producing similar kinase activities *in vivo* should exhibit different sensitivities to ligand in proportion to the extent of methylation required to maintain a wild-type rotational bias. Our results support this hypothesis and are consistent with the proposed mechanism of adaptive modification (*55*). VB13 (*cheR*$^+$*B*$^+$) cells expressing Tar WY-2 through WY+1 possess similar rotational biases (Figure 2) and MRFs (Figure 3.3) suggesting similar levels of *in vivo* kinase stimulation. However, these receptors require different levels of methylation to maintain wild-type rotational biases (Figure 3.5). As hypothesized, we discovered that the sensitivities to a gradient of attractant decreased (Figure 3.6A) as the extent of methylation (Figure 3.5) required to maintain wild-type levels of kinase stimulation *in vivo* (Figure 3.2) increased. In addition, analyses performed in the absence of adaptive

modification (Figures 3.6B and 3.6C), support its role in maintaining the relationship between level of methylation, receptor signaling state, and ligand sensitivity. These observations highlight the enormous restorative power of covalent receptor methylation and underscore the robustness of the adaptation machinery.

Discussion

Binding of aspartate to the periplasmic domain of the Tar chemoreceptor is proposed to displace the second transmembrane helix (TM2), which connects the periplasmic and cytoplasmic domains of the protein, a few ångströms toward the cytoplasm (*38-44*). This displacement repositions TM2 relative to the plane of the phospholipid bilayer. Therefore, interactions of TM2 with the membrane may be critical for setting the baseline signaling state of the receptor. Arginine-scanning mutagenesis of *Salmonella* Tar revealed the importance of aromatic residues within TM2. Substitution of Phe-189 or Trp-192 stabilized the "on"-state of Tar, while substitution of Trp-209 promoted the "off" conformation (*42*). We previously showed that Trp-209 and, to a lesser extent, Tyr-210 help maintain the normal baseline-signaling state of *E. coli* Tar (*43*). Here, we extended our previous analysis by systematically moving the Trp-209/Tyr-210 aromatic pair in single-residue steps to precisely modulate the signaling character of Tar. In the context of an intact chemotactic circuit (*i.e.*, in *cheR*$^+$*B*$^+$ cells), this manipulation allows us to "tune" the signaling properties of Tar in a predictable manner. To our knowledge, this is the first time that protein-membrane interactions have

been harnessed to incrementally manipulate the signaling state of a transmembrane receptor over its full range of activities.

A chemoreceptor must process several allosteric inputs, including ligand occupancy, extent of covalent methylation, and higher-order interactions with other chemoreceptors. The "frozen dynamic" model for modulation of CheA activity (*28, 30*) suggests that allosteric inputs change the supercoiling state of a four-helix bundle composed of a coiled-coil of two anti-parallel helices from each monomer. In the "off" (attractant-bound) state the receptor has more conformational freedom, whereas in the "on" (repellent-bound) state the four-helix bundle is less dynamic. The adaptation sub-domain forms a four-helix bundle that is contiguous with the signaling sub-domain (*65*). The four Glu residues that are subject to covalent modification by the CheR methyltransferase may act as an "electrostatic switch." Neutralization of the negative charges on these residues, corresponding to methylation *in vivo*, should decrease electrostatic repulsion between the two subunits of a homodimer, resulting in decreased mobility of the signaling domain and increased levels of kinase stimulation (Figure 3.7A) (*66, 67*). The HAMP-linker connects TM2 to the adaptation and signaling sub-domains. In some fashion, it must transduce vertical displacements of TM2 into changes in helical supercoiling of the cytoplasmic domain.

The steady-state *in vivo* kinase activities, reflected in the rotational biases of tethered cells, associated with the mutant receptors are affected by allosteric contributions from both ligand-occupancy and adaptive methylation. Therefore, receptors with different, but still balanced, contributions of ligand-binding and adaptive

Figure 3.7. Adaptive methylation allows mutant Tar receptors to support similar baseline CheA activities. (A) The "frozen dynamic" model for modulation of CheA activity (*28, 30*) suggests that allosteric inputs change the supercoiling state of the signaling sub-domain, which forms a contiguous four-helix bundle with the adaptation sub-domain (*67*). Neutralization by methylation of negatively charged Glu residues within the adaptation sub-domain decreases electrostatic repulsion between the two subunits of a homodimer, resulting in decreased mobility of the signaling domain and increased levels of kinase stimulation (*66*). This degree of mobility is illustrated as differential spacing between the methylation domains within a Tar homodimer, with a larger spacing indicating higher mobility. In its adapted state, a receptor is in an intermediate signaling state, which leads to CW/CCW flagellar rotation (center). This state may represent equilibrium between fully "on" (left; exclusively CW flagellar rotation) and fully "off" (right; exclusively CCW flagellar rotation) states. Attractant binding may displace TM2 into the cytoplasm (right), as indicated by a downward-facing arrow, to produce a localized membrane deformation. The polar regions of the lipid bilayer are represented in dark gray, whereas the hydrophobic core shown in light gray. The amphipathic aromatic residues near the periplasmic (Trp-192) and cytoplasmic (Trp-209/Tyr-210) ends of TM2 are represented as red boxes. Note that only one TM2 is shown as displaced to account for the asymmetry of attractant-induced signaling (*54, 55*), although both of the HAMP linkers of the dimer are probably affected, as illustrated. Repellent binding may displace TM2 toward the periplasm as indicated by an upward-facing arrow. For sake of consistency, repellent signaling is also illustrated as asymmetric, although this has not been demonstrated experimentally. Adaptive methylation and demethylation are envisioned as returning attractant-bound and repellent-bound receptors, respectively, to the intermediate (CW/CCW) signaling state. (B) Repositioning of TM2 by moving the tandem Trp-209/Tyr-210 residues may generate conformational changes similar to those that occur when an attractant or a repellent interacts with the receptor. For relatively small displacements (WY-1 and -2, and WY+1), which may correspond to attractant-induced and repellent-induced conformational changes, respectively, the methylation system can compensate to restore nearly normal levels of CheA kinase stimulation *in vivo*. We suggest that repositioning the Trp-Tyr pair produces TM2 displacements that change the distance between of beginning of the HAMP domain and the inner leaflet of membrane. In the case of the plus-series receptor mutants, the distance decreases (as may happen in response to repellent binding), whereas within the minus-series of receptors this distance would increase (as is thought to happen in response to attractant binding). The displacements of TM2 in WY-3, WY+2, and WY+3 Tar are too large to be completely compensated by adaptive methylation or demethylation. Therefore, these receptors are strongly biased toward the "off" state (WY-3, right) or the "on" state (WY+2 and +3, left). Note that both TM2s are displaced within the dimer, unlike the asymmetrical displacement of TM2 by attractant or repellent binding as shown in (A).

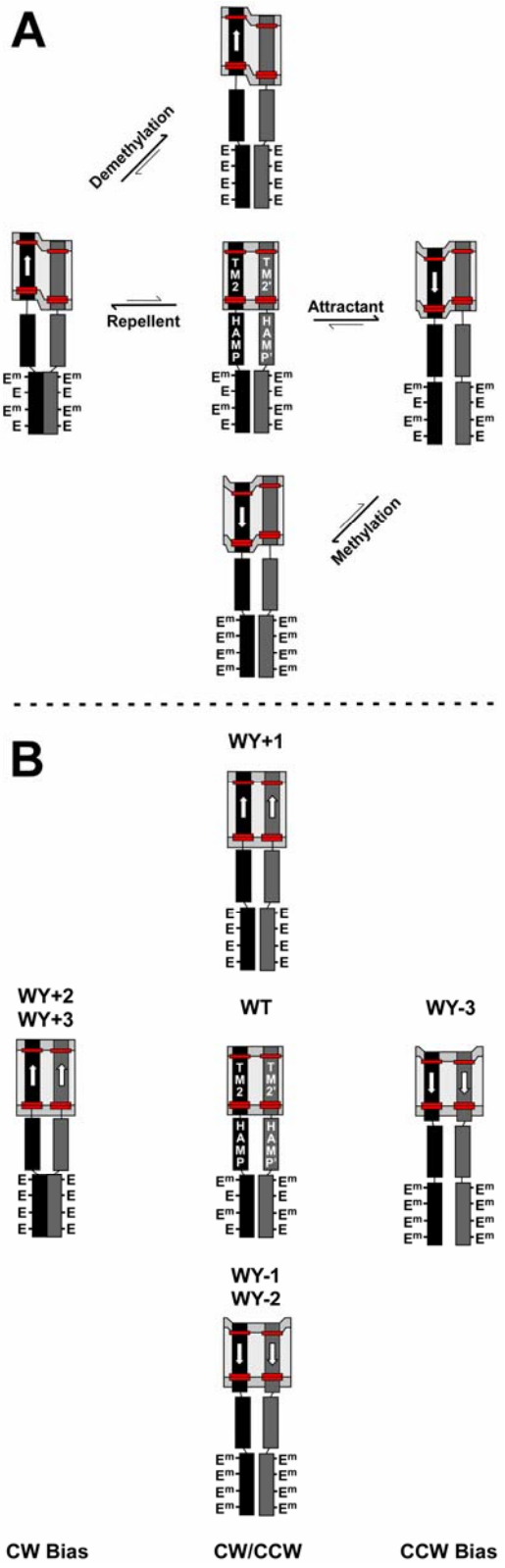
A
Demethylation
Repellent
Attractant
Methylation
TM2
TM2'
HAMP
HAMP'
B
WY+1
WY+2
WY+3
WT
WY-3
WY-1
WY-2
CW Bias
CW/CCW
CCW Bias

methylation can possess similar activities (Figure 3.7B). Tar WY-2, Tar WY-1, wild-type Tar, and Tar WY+1 produce similar rotational phenotypes (Figure 3.2) and mean reversal frequencies (Figure 3.3) in *cheR*$^+$*B*$^+$ cells, suggesting that they possess equivalent abilities to stimulate CheA *in vivo*. However, each of these receptors is in a different signaling state that reflects changes that are induced by repositioning TM2 and compensated by adaptive methylation (Figure 3.7B). WY-2 and WY-1 Tar exhibit increased levels of methylation (Figure 3.5). Conversely, WY+1 is less methylated (Figure 3.5). Even though tethered *cheR*$^+$*B*$^+$ cells expressing these mutant receptors have nearly identical CW/CCW ratios of flagellar rotation, the corresponding swimming cells show decreased sensitivity in the chemotaxis swarm assay (Figure 3.6A).

Methylation of MCPs in receptor/CheA/CheW ternary complexes has been suggested to cause adaptation by altering the gain between ligand binding and kinase inhibition (*72*). Therefore, we predicted that the mutant receptors would possess differences in sensitivity to a gradient of ligand. The results (Figure 3.6A) support our hypothesis and suggest that when Trp-209/Trp-210 are at their original positions the receptor possesses a level of methylation *in vivo* that allows optimal sensitivity to a gradient of attractant.

Tar WY-3 possesses the largest displacement of TM2 toward the cytoplasm and produces CCW-biased behavior even in *cheR*$^+$*B*$^+$ tethered cells (Figure 3.2). In this case, adaptive methylation cannot restore a normal CW/CCW rotational bias. The majority of tethered cells expressing WY+2 and WY+3 Tar exhibit a CW-biased rotational phenotype (Figure 3.2), suggesting that they also have a displacement of TM2, albeit in

the opposite direction, that cannot be fully compensated by demethylation. A subpopulation of *cheR*$^+$*B*$^+$ cells producing these proteins rotate their flagella exclusively CCW, suggesting that in some cells the population of mutant receptors is primarily in an inactive state. Presumably, larger displacements of TM2 toward the periplasm tend to distort Tar into a conformation in which it is unable to stimulate CheA. Our results clearly demonstrate that there are limits to the extent to which TM2 can be repositioned while retaining normal Tar function. The changes conferred by WY-3, WY+2, and WY+3 Tar cannot be compensated by the methylation/demethylation system, suggesting that in these receptors TM2 is displaced outside its normal range of motion (Figure 3.7B).

The rotational biases (Figure 3.4) and mean reversal frequencies (Figure 3.3) caused by repositioning the Trp/Tyr pair are not graded when the mutant receptors are expressed in Δ*cheRB* cells. The same is true when the mutant receptors are analyzed in the *in vitro* assay for receptor-coupled CheA kinase activity. In the latter assay, the WY-1 through WY-3 receptors all stimulated CheA very weakly (Figure 3.6B). The WY+1 through WY+3 receptors all stimulated CheA significantly, although Tar WY+2 and WY+3 were considerably less active than wild-type Tar. The most notable difference, however, was in the response to titration by aspartate. The aspartate K_i was somewhat higher for all three mutant proteins, but the biggest difference was in the apparent cooperativity of the inhibition. For wild-type Tar, the apparent Hill coefficient was 1.8, whereas for the WY+1 through WY+3 receptors the apparent Hill coefficient fell to 0.2 (Figure 3.6C). We do not know whether the increased K_i and decreased cooperativity

reflect a lower affinity for aspartate, a partial decoupling of ligand binding and receptor inhibition, or some combination of these effects. The WY-1 to WY-3 receptors, which are inactive in their QEQE forms, may stimulate kinase activity when present in their QQQQ forms, which are equivalent to fully methylated receptors. Conversely, the EEEE forms of WY+1 to WY+3 Tar may exhibit a pattern of aspartate inhibition more like that of QEQE Tar.

Several functional chimeric receptors have been made by fusing the periplasmic, transmembrane, and HAMP-linker domains of chemoreceptors to the signaling domains of sensor kinases (*101, 102*), and *vice versa* (*103*), suggesting that the mechanism of signal transduction is conserved for these related proteins. Thus, we predict that mutations in transmembrane sensor kinases analogous to the ones described here could generate a graded series of signaling outputs, without the complication of adaptive methylation. Chemoreceptors have also been modified to confer different ligand specificity (*110, 111*). A combinatorial approach has been used with the bacterial periplasmic binding protein (bPBP) superfamily (*112*) to create chemoreceptors that interact with a broad range of ligands that cannot bind directly to the transmembrane receptors. Modification of any of the allosteric contributions to signaling by such "rationally designed" proteins, including changes to TM2, the HAMP linker, and the adaptation sub-domain, can be used, in principle, to tune their activities.

The solution structure of the HAMP domain of a hyperthermophilic archae was recently determined (*61*) using nuclear magnetic resonance (NMR) spectroscopy. The authors suggest that helical rotations within a parallel coiled-coil domain are responsible

for signal propagation. They conclude that their results imply that a piston-type displacement of TM2 cannot be responsible for transmembrane signal transduction (*38-44*). Everyone in the field of transmembrane signaling should be excited about the determination of the structure of a soluble HAMP domain. However, the HAMP domain used in this study was hardly typical, which may explain the authors' success in the structural determination of one possible conformation. Furthermore, potential protein-membrane interactions are absent in aqueous solution. We therefore advise caution in drawing sweeping conclusions from valuable, but necessarily limited, data.

CHAPTER IV

GENERAL CONCLUSIONS AND FUTURE DIRECTIONS

Summary

Membrane-spanning receptors detect extracellular stimuli and communicate that information to the cell interior. *E. coli* chemoreceptors use a small (~1-3Å) piston-like displacement of TM2 toward the cytoplasm to signal attractant binding (*38-44*). The research presented in this dissertation examines the role of protein-membrane interactions during transmembrane signaling by the aspartate chemoreceptor (Tar). It begins by examining the contribution of residues within TM2 to the signaling state of Tar. Residues at the cytoplasmic polar-hydrophobic interface of the cellular membrane (*42*), namely Trp-209 and Tyr-210, were found to be critical for maintenance of a normal baseline signaling state (Chapter II). Furthermore, repositioning this tandem pair in single-residue steps about their original position was shown to modulate the signaling state of Tar in an incremental manner (Chapter III).

Trp-209 and Tyr-210 contribute to the baseline signaling state of Tar

Phospholipid bilayers consist of polar, hydrophilic regions that flank a central nonpolar, hydrophobic core. To minimize energetically unfavorable protein-membrane interactions, specific amino acids occupy different positions within a transmembrane α helix. A transmembrane helix typically consists of a central core of aliphatic residues flanked by amphipathic aromatic residues at the polar-hydrophobic interface and charged residues at the membrane-water interface (*79*). TM2 of *E. coli* Tar conforms to

this consensus motif (Figure 1.4B) (*42*). During the initial study, I examined the contribution of Trp residues because synthetic peptides consisting of an Ala-Leu core of different lengths flanked by Trp (WALP peptides) (*81*) interact with phospholipid bilayers in a characteristic manner. The flanking Trp residues exhibit a very strong tendency to remain within the interfacial region regardless of the length of hydrophobic mismatch (*64*). The flanking Trp residues exhibit a very strong tendency to remain within the interfacial region regardless of the length of hydrophobic mismatch (*64*). Hydrophobic mismatch occurs when the length of the aliphathic residues within a transmembrane helix is different than the thickness of the hydrophobic core of the lipid bilayer it passes through. Previously, hydrophobic mismatch was thought to be the dominant element in determining how transmembrane helices interact with their lipid environment. This result demonstrates that Trp residues play a more significant role in positioning α helices within a membrane.

I began by substituting alanyl residues for Trp-192 and Trp-209. Substitution of Trp-192 resulted in no change in the baseline signaling state of Tar. However, cells expressing Tar W209A possessed a baseline signaling state that was severely biased toward the kinase-inhibiting conformation (Figure 2.2 and Table 2.2). These results suggest that the W209A substitution may cause the C-terminus of TM2 to protrude farther into the cytoplasm, in a manner similar to the displacement observed upon binding of aspartate (Figure 2.4). By repositioning Trp-209 about its original position, we also determined that Tyr-210 plays an accessory role in maintaining TM2 position within the membrane.

Harnessing TM2-membrane interactions to modulate Tar signal output

I extended the initial analysis by systemically moving the Trp-209/Tyr-210 pair in single-residue steps in either direction. In the context of an intact chemotactic circuit, this manipulation allowed us to "tune" the signaling properties of Tar in a predictable manner. The result was the production of a series of transmembrane receptors with incrementally modulated signaling states spanning the entire range of possible receptor activities.

These results demonstrate that the steady-state *in vivo* kinase activities associated with mutant receptors are affected by the allosteric contribution from both ligand-occupancy and adaptive methylation. Receptors with different, but still balanced, contributions of ligand-binding and adaptive methylation can possess similar *in vivo* activities (Figure 3.7B). Tar WY-2, Tar WY-1, wild-type Tar, and Tar WY+1 produce similar rotational phenotypes (Figure 3.2) and mean reversal frequencies (Figure 3.3) in *cheR*$^+$*B*$^+$ cells, suggesting that they possess equivalent abilities to stimulate CheA *in vivo*. However, each of these receptors is in a different signaling state that reflects changes that are induced by repositioning TM2 and compensated by adaptive methylation. WY-2 and WY-1 Tar exhibit increased levels of methylation relative to wild-type Tar (Figure 3.5). Conversely, WY+1 Tar is less methylated (Figure 3.5). The results also show that there are limits to the extent to which TM2 can be repositioned and still retain normal Tar function. The changes conferred by the WY-3, WY+2, and WY+3 repositionings cannot be compensated by the methylation/demethylation system,

suggesting that in these receptors TM2 is displaced outside its normal range of motion (Figure 3.7B).

The results support a recent model for methylation of receptors in ternary complexes with CheA and CheW. Methylation has been suggested to cause adaptation by altering the gain between ligand binding and kinase inhibition (*72*). Even though tethered *cheR*$^+$*B*$^+$ cells expressing these mutant receptors have nearly identical CW/CCW ratios of flagellar rotation (Figure 3.2), the corresponding swimming cells show decreased sensitivity in the chemotaxis swarm assay (Figure 3.6A). Therefore, we identified an inverse correlation between the extent of adaptive methylation required to maintain a normal rotational bias in tethered cells and the sensitivity of cells expressing these receptors to a gradient of attractant.

Examining signal processing by the HAMP domain

One logical extension of this research would be to analyze HAMP domain function in mutant receptors with biased signaling states. HAMP domains transduce extracellular sensory input into an intracellular signaling response in over 7500 proteins, including chemoreceptors and sensor histidine kinases (*61*). Within most transmembrane receptors, these domains reside adjacent to the inner leaflet of the cytoplasmic membrane (*45*). HAMP domains consist of two amphipathic α helical sequences (AS1 and AS2) connected by a short flexible linker (*58-60*). As discussed extensively in Chapter I, two models of the role of the HAMP linker in signal transduction have been proposed: a “helix interaction” model, involving peripheral association of AS1 with the

membrane (*60*) (Figure 1.5A), and a second implying changes in helical register within a parallel coiled-coil domain (*61*) (Figure 1.5B). It remains possible that both models are correct and that they are used within different classes of receptors. Another possibility is that the two models may represent alternative HAMP conformations within a single receptor.

To determine whether these models reflect reality and to identify potential HAMP-membrane interactions, genes encoding mutant Tar proteins that possess intermediate swarm rates (Tar WY-2 and WY+1) could be used as templates for random mutagenesis of AS1. Rapid screening of cells in semisolid swarm agar should yield a variety of suppressing mutations that restore a wild-type swarm rate. If the "helix interaction" model is correct, residue substitutions within AS1 predicted to increase interaction with the inner leaflet of the membrane (introduction of aromatic, hydrophobic, or positively charged residues) would be expected to shift the equilibrium toward the kinase-stimulating state, whereas those predicted to reduce interaction with the membrane (introduction of polar or negatively-charged residues) would be expected to bias the equilibrium toward the kinase-inhibiting state. The position of the substituted residues should also be considered in the context of the solution structure of an archaeal HAMP domain (*61*). Using two mutant receptors that possess signaling states biased in opposite directions in this study may result in isolation of sets of suppressing mutations of opposite natures. This approach will require a large collection of suppressors for each type of mutant receptor.

Application to other two-component signaling pathways

Another logical extension of this research would be to establish a method to examine a wide range of two-component signaling pathways controlled by transmembrane receptors. One prevalent type of environmental sensor in prokaryotic organisms is the two-component system (TCS). A recent survey of 145 prokaryotic genomes detected more than 4000 TCSs (*113*). TCSs regulate a diverse array of virulence factors (*114, 115*). A canonical TCS consists of a membrane-spanning sensor histidine kinase (SHK) and a cytoplasmic response regulator (RR). Understanding two-component signaling pathways that lead to enhanced pathogenicity is essential for understanding complex host-pathogen interactions and could result in the detection of previously unidentified therapeutic targets. The research presented within this dissertation demonstrates that moving the tandem Trp/Tyr residues near the cytoplasmic end of TM2 can be used to "tune" the signal output of Tar in predictable steps (*44*). Aromatic residues are located near the cytoplasmic end of TM2 within many SHKs (*43*) (Figure 2.6), in which they may control the signaling state of the SHK.

A four-tiered approach could be used to establish a method to identify and harness SHK-membrane interactions to modulate SHK output in a controlled manner. Directly manipulating SHK output would provide a technique to study two-component signaling systems without knowing the precise signal-eliciting ligand. First, potential SHK-membrane interactions could be examined in a few select SHKs. Two of the most well-characterized, EnvZ and NarX, are predicted (using TMHMM; *116, 117*) to share a distribution of charge and aromaticity in TM2 that is similar to that in Tar (*42*). If the

mechanism of transmembrane signaling is conserved between SHKs and chemoreceptors, repositioning aromatic residues about the cytoplasmic polar-hydrophobic interface within EnvZ and NarX may modulate their signaling output in a manner similar to what was observed with Tar. Previously described (*118, 119*) transcriptional and translational reporter systems could be used to monitor changes in signal output upon repositioning of these residues in EnvZ (Trp-176/Phe-178) and NarX (Trp-173). If no correlation is observed, alanine-scanning mutagenesis could be used to determine whether neighboring residues within TM2 contribute to the baseline signal output of EnvZ and NarX.

After important TM2-membrane interactions have been identified, functional Tar-SHK chimeras could be created. Multiple fusion sites would need to be investigated to elucidate the relationship between TM2 and the HAMP domain and to maximize the probability of creating a fully functional Tar-NarX chimera (Figure 4.1). The fusion joint in the first chimera should be prior to TM2. This region should tolerate substitutions, and the distance between TM2 and the HAMP domain of NarX will remain constant. The second fusion joint should be after the conserved Arg residue at the cytoplasmic end of TM2. This fusion may change the distance between the end of Tar TM2 and the beginning of NarX AS1. The final fusion joint should be C-terminal to the HAMP domain, so that the hybrid contains the entire Tar HAMP domain joined to the remainder of the cytoplasmic portion of NarX. The activities supported by NarX and Tar-NarX chimeras in the absence and presence of nitrate and aspartate, respectively, will define basal and ligand-induced signal outputs. This comparison may determine whether the

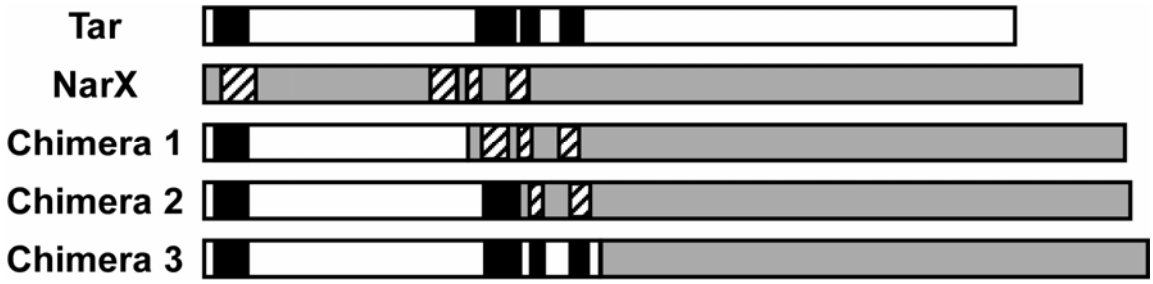

Figure 4.1. Chimeric Tar-NarX receptors. Tar and NarX are depicted in white and gray, respectively. From left to right, the black boxes within Tar or the diagonally-striped boxes within NarX represent TM1, TM2, AS1, and AS2. Chimera 1 contains the TM2 and HAMP domains from NarX. The second chimeric protein contains TM2 of Tar and the HAMP domain of NarX. The final chimera possesses the TM2 and HAMP domain of Tar.

displacement of TM2 produced by aspartate is similar to that produced by nitrate and which combination of TM2 and HAMP domains should be considered for other Tar-SHK chimeras.

Next, the output of Tar-SHK chimeras could be modulated by altering the interactions between TM2 and the membrane. Previous results with a NarX-Tar chimera (Nart; *103*) suggest chimeric proteins similar to those proposed here retain both the essential properties of their individual domains and the ability of the domains to conformationally communicate. Nart was shown to retain a correlation between liagnd-occupancy and signal output while retaining sensitivity to ligand. Based on these results, a total of three Tar-NarX and three Tar-EnvZ chimeras should be studied: an "off" chimera that supports minimal RR phosphorylation; a "baseline" chimera with intermediate activity; and an "on" chimera that produces maximal RR phosphorylation. The signal outputs of these proteins could be analyzed to determine the feasibility of introducing the C-termini of other SHKs into the system. The functional interactions between the SHKs and RRs of *E. coli* have been characterized in an *in vitro* phosphorylation assay (*120*) that provides enough information to create reporter constructs for all SHKs. This systems-level analysis would categorize the mechanism of transmembrane signaling by each SHK into one of three classes: SHKs that transduce signal by TM2 displacement toward the cytoplasm; those that signal by TM2 displacement toward the periplasm; and those that utilize an entirely different mechanism such as rotation of TM2 relative to TM1 (*121*).

The final objective of this research would be to couple chimeric expression systems with transcriptional profiling to identify the targets of TCSs in any organism. Transcriptional profiles of *E. coli* cells expressing an "off" chimera could be compared with those expressing an "on" chimera to determine which genes are subject to regulation upon changes in SHK output. One advantage of this approach would be that the signal-eliciting ligand would not have to be known. After comparing the differences in output among cells expressing these receptors, aspartate could be used to modulate the activity of the intermediate (or "baseline") Tar-SHK chimera to confirm that the differences are dependent on ligand-induced changes in SHK signal output.

Predicting dynamic transmembrane-helix movements *in silico*

A final application of this research would involve a synergistic approach using experimental and computational techniques. As described above, creation and analysis of Tar-SHK chimeras with harnessed TM2-membrane interactions may classify transmembrane signaling by SHKs into one of three groups: a displacement of TM2 toward the periplasm; a displacement toward the cytoplasm; or using a different mechanism (*i.e.* rotation of TM2).

Recently, a "biological" hydrophobicity scale was published (*122*) that approximated the propensity for each amino acyl residue to promote insertion of a poly-Ala α helix into a biological membrane. The apparent free energies of membrane insertion were calculated for all 20 amino acyl residues at different positions. These free energies were found to be additive; therefore, a computational analysis of the primary

sequence within and flanking TM2 could be compared to the experimentally determined parameters of mechanism of transmembrane signaling. One would expect different residues to be present at different positions within a membrane-spanning helix based on the mechanism employed. For example, an SHK that conveys the presence of extracellular ligand by rotation might be predicted to have a greater resistance to removal from the membrane when compared to an SHK that signals by displacement.

These experiments would provide a conceptual framework for predicting transmembrane helix movement within intact proteins. The ability to these movements would be very useful for analyzing SHKs, or other proteins, with dynamic transmembrane helices.

Overall application of this research

The experiments suggested here describe a potential method for manipulation of transmembrane proteins. A systematic method for engineering the signaling parameters of fully functional transmembrane receptors (*e.g.* SHKs) would have broad implications in research involving two-component signaling pathways. This approach could also be used to modulate the signaling parameters of novel biosensors that use SHKs as protein scaffolds (*111, 112*).

REFERENCES

1. Adler, J. (1966) Chemotaxis in bacteria, *Science 153,* 708-16.

2. Tso, W. W., and Adler, J. (1974) Negative chemotaxis in *Escherichia coli*, *J. Bacteriol. 118*, 560-76.

3. Bibikov, S. I., Biran, R., Rudd, K. E., and Parkinson, J. S. (1997) A signal transducer for aerotaxis in *Escherichia coli*, *J. Bacteriol. 179*, 4075-9.

4. Rebbapragada, A., Johnson, M. S., Harding, G. P., Zuccarelli, A. J., Fletcher, H. M., Zhulin, I. B., and Taylor, B. L. (1997) The Aer protein and the serine chemoreceptor Tsr independently sense intracellular energy levels and transduce oxygen, redox, and energy signals for *Escherichia coli* behavior, *Proc. Natl. Acad. Sci. U.S.A. 94*, 10541-6.

5. Mesibov, R., and Adler, J. (1972) Chemotaxis toward amino acids in *Escherichia coli*, *J. Bacteriol. 112*, 315-26.

6. Adler, J., Hazelbauer, G. L., and Dahl, M. M. (1973) Chemotaxis toward sugars in *Escherichia coli*, *J. Bacteriol. 115*, 824-47.

7. Manson, M. D., Blank, V., Brade, G., and Higgins, C. F. (1986) Peptide chemotaxis in *E. coli* involves the Tap signal transducer and the dipeptide permease, *Nature 321*, 253-6.

8. Khan, S., Pierce, D., and Vale, R. D. (2000) Interactions of the chemotaxis signal protein CheY with bacterial flagellar motors visualized by evanescent wave microscopy, *Curr. Biol. 10,* 927-30.

9. Berg, H. C., and Anderson, R. A. (1973) Bacteria swim by rotating their flagella filaments, *Nature 245,* 380-2.

10. Silverman, M., and Simon, M. (1974) Flagellar rotation and the mechanism of bacterial motility, *Nature 249*, 73-4.

11. Turner, L., Ryu, W. S., and Berg, H. C. (2000) Real-time imaging of fluorescent flagellar filaments, *J. Bacteriol. 182*, 2793-801.

12. Macnab, R. M., and Koshland, D. E. Jr (1972) The gradient-sensing mechanism in bacterial chemotaxis, *Proc. Natl. Acad. Sci. U.S A. 69,* 2509-12.

13. Brown, D. A., and Berg, H. C. (1974) Temporal stimulation of chemotaxis in *Escherichia coli*, *Proc. Natl. Acad. Sci. U.S.A. 71,* 1388-92.

14. Segall, J. E., Block, S. M., and Berg, H. C. (1986) Temporal comparisons in bacterial chemotaxis, *Proc. Natl. Acad. Sci. U.S.A. 83*, 8987-91.

15. Borkovich, K. A., Kaplan, N., Hess, J. F., and Simon, M. I. (1989) Transmembrane signal transduction in bacterial chemotaxis involves ligand-dependent activation of phosphate group transfer, *Proc. Natl. Acad. Sci. U.S.A. 86*, 1208-12.

16. Hess, J. F., Oosawa, K., Kaplan, N., and Simon, M. I. (1988) Phosphorylation of three proteins in the signaling pathway of bacterial chemotaxis, *Cell 53*, 79-87.

17. Ravid, S., Matsumura, P., and Eisenbach, M. (1986) Restoration of flagellar clockwise rotation in bacterial envelopes by insertion of the chemotaxis protein CheY, *Proc. Natl. Acad. Sci. U.S.A. 83*, 7157-61.

18. Welch, M., Oosawa, K., Aizawa, S., and Eisenbach, M. (1993) Phosphorylation-dependent binding of a signal molecule to the flagellar switch of bacteria, *Proc. Natl. Acad. Sci. U.S.A. 90*, 8787-91.

19. Cluzel, P., Surette, M., and Leibler, S. (2000) An ultrasensitive bacterial motor revealed by monitoring signaling proteins in single cells, *Science 287*, 1652-5.

20. Borkovich, K. A., and Simon, M. I. (1990) The dynamics of protein phosphorylation in bacterial chemotaxis, *Cell 63*, 1339-48.

21. Goy, M. F., Springer, M. S., and Adler, J. (1977) Sensory transduction in *Escherichia coli*: role of a protein methylation reaction in sensory adaptation, *Proc. Natl. Acad. Sci. U.S.A. 74*, 4964-8.

22. Springer, W. R., and Koshland, D. E., Jr. (1977) Identification of a protein methyltransferase as the *cheR* gene product in the bacterial sensing system, *Proc. Natl. Acad. Sci. U.S.A. 74*, 533-7.

23. Stock, J. B., and Koshland, D. E., Jr. (1978) A protein methylesterase involved in bacterial sensing, *Proc. Natl. Acad. Sci. U.S.A. 75*, 3659-63.

24. Lupas, A., and Stock, J. (1989) Phosphorylation of an N-terminal regulatory domain activates the CheB methylesterase in bacterial chemotaxis, *J. Biol. Chem. 264*, 17337-42.

25. Bornhorst, J. A., and Falke, J. J. (2000) Attractant regulation of the aspartate receptor-kinase complex: limited cooperative interactions between receptors and effects of the receptor modification state, *Biochemistry 39*, 9486-93.

26. Li, G., and Weis, R. M. (2000) Covalent modification regulates ligand binding to receptor complexes in the chemosensory system of *Escherichia coli*, *Cell 100*, 357-65.

27. Goy, M. F., Springer, M. S., and Adler, J. (1978) Failure of sensory adaptation in bacterial mutants that are defective in a protein methylation reaction, *Cell 15*, 1231-40.

28. Kim, K. K., Yokota, H., and Kim, S. H. (1999). Four-helical-bundle structure of the cytoplasmic domain of a serine chemotaxis receptor, *Nature 400*, 787-92.

29. Kim, S. H., Wang, W., and Kim, K. K. (2002). Dynamic and clustering model of bacterial chemotaxis receptors: structural basis for signaling and high sensitivity, *Proc. Natl. Acad. Sci. U.S.A. 99*, 11611-5.

30. Kim, S. H. (1994). "Frozen" dynamic dimer model for transmembrane signaling in bacterial chemotaxis receptors, *Protein Sci. 3*, 159-65.

31. Shrout, A. L., Montefusco, D. J., and Weis, R. M. (2003) Template-directed assembly of receptor signaling complexes, *Biochemistry 42*, 13379-85.

32. Springer, M. S., Goy, M. F., and Adler, J. (1977) Sensory transduction in *Escherichia coli*: two complementary pathways of information processing that involve methylated proteins, *Proc. Natl. Acad. Sci. U.S.A. 74*, 3312-6.

33. Tam, R., and Saier, M. H., Jr. (1993) Structural, functional, and evolutionary relationships among extracellular solute-binding receptors of bacteria, *Microbiol. Rev. 57,* 320-46.

34. Quiocho, F. A. (1990) Atomic structures of periplasmic binding proteins and the high-affinity active transport systems in bacteria, *Philos. Trans. R. Soc. Lond. B. Biol. Sci. 326,* 341-51.

35. Milburn, M. V., Prive, G. G., Milligan, D. L., Scott, W. G., Yeh, J., Jancarik, J., and Koshland, D. E., Jr., and Kim, S. H. (1991) Three-dimensional structures of the ligand-binding domain of the bacterial aspartate receptor with and without a ligand, *Science 254*, 1342-7.

36. Spurlino, J. C., Lu, G.-Y., and Quiocho, F. A. (1991) The 2.3-Å resolution structure of the Maltose- or Maltodextrin-binding protein, a primary receptor of bacterial active transport and chemotaxis, *J. Biol. Chem. 266,* 5202-19.

37. Zhang, Y., Gardina, P. J., Kuebler, A. S., Kang, H. S., Christopher, J. A., and Manson M. D. (1999) Model of maltose-binding protein/chemoreceptor complex supports intrasubunit signaling mechanism, *Proc. Natl. Acad. Sci. U.S.A. 96,* 939-44.

38. Chervitz, S. A., and Falke, J. J. (1995) Lock on/off disulfides identify the transmembrane signaling helix of the aspartate receptor, *J. Biol. Chem. 270*, 24043-53.

39. Hughson, A. G., and Hazelbauer, G. L. (1996) Detecting the conformational change of transmembrane signaling in a bacterial chemoreceptor by measuring effects on disulfide cross-linking *in vivo*, *Proc. Natl. Acad. Sci. U.S.A. 93,* 11546-51.

40. Ottemann, K. M., Xiao, W., Shin, Y. K., and Koshland, D. E., Jr. (1999) A piston model for transmembrane signaling of the aspartate receptor*, Science 285*, 1751-4.

41. Isaac, B., Gallagher, G. J., Balazs, Y. S., and Thompson, L. K. (2002) Site-directed rotational resonance solid-state NMR distance measurements probe structure and mechanism in the transmembrane domain of the serine bacterial chemoreceptor, *Biochemistry 41*, 3025-36.

42. Miller, A. S., and Falke, J. J. (2004) Side chains at the membrane-water interface modulate the signaling state of a transmembrane receptor, *Biochemistry 43*, 1763-70.

43. Draheim, R. R., Bormans, A. F., Lai, R.-Z., and Manson, M. D. (2005) Tryptophan residues flanking the second transmembrane helix (TM2) set the signaling state of the Tar chemoreceptor, *Biochemistry 44*, 1268-77.

44. Draheim, R. R., Bormans, A. F., Lai, R.-Z., and Manson, M. D. (2006) Tuning a bacterial chemoreceptor with protein-membrane interactions, *Biochemistry 45*, 14655-64.

45. Ulrich, L. E., and Zhulin, I. B. (2005) Four-helix bundle: a ubiquitous sensory module in prokaryotic signal transduction, *Bioinformatics 21 Suppl 3,* 45-8.

46. Yeh, J. I., Biemann, H. P., Prive, G. G., Pandit, J., Koshland, D. E., Jr., and Kim, S. H. (1996) High-resolution structures of the ligand binding domain of the wild-type bacterial aspartate receptor, *J. Mol. Biol. 262*, 186-201.

47. Bowie, J. U., Pakula, A. A., and Simon, M. I. (1995) The three-dimensional structure of the aspartate receptor from *Escherichia coli*, *Acta. Crystallogr., Sect. D 51*, 145-54.

48. Falke, J. J., and Koshland, D. E., Jr. (1987) Global flexibility in a sensory receptor: a site-directed cross-linking approach, *Science 237*, 1596-600.

49. Milligan, D. L., and Koshland, D. E., Jr. (1988) Site-directed cross-linking. Establishing the dimeric structure of the aspartate receptor of bacterial chemotaxis, *J. Biol. Chem. 263*, 6268-75.

50. Lynch, B. A., and Koshland, D. E., Jr. (1991) Disulfide cross-linking studies of the transmembrane regions of the aspartate sensory receptor of *Escherichia coli*, *Proc. Natl. Acad. Sci. U.S.A. 88*, 10402-6.

51. Pakula, A. A., and Simon, M. I. (1992) Determination of transmembrane protein structure by disulfide cross-linking: the *Escherichia coli* Tar receptor, *Proc. Natl. Acad. Sci. U.S.A. 89*, 4144-8.

52. Stoddard, B. L., Bui, J. D., and Koshland, D. E., Jr. (1992) Structure and dynamics of transmembrane signaling by the *Escherichia coli* aspartate receptor, *Biochemistry 31*, 11978-83.

53. Scott, W. G., and Stoddard, B. L. (1994) Transmembrane signalling and the aspartate receptor, *Structure 2*, 877-87.

54. Gardina, P. J., and Manson, M. D. (1996) Attractant signaling by an aspartate chemoreceptor dimer with a single cytoplasmic domain, Science *274*, 425-6.

55. Tatsuno, I., Homma, M., Oosawa, K., and Kawagishi, I. (1996) Signaling by the *Escherichia coli* aspartate chemoreceptor Tar with a single cytoplasmic domain per dimer, Science *274*, 423-5.

56. Biemann, H. P., and Koshland, D. E., Jr. (1994) Aspartate receptors of *Escherichia coli* and *Salmonella typhimurium* bind ligand with negative and half-of-the-sites cooperativity, *Biochemistry 33*, 629-34.

57. Lai, W. C., Beel, B. D., and Hazelbauer, G. L. (2006) Adaptational modification and ligand occupancy have opposite effects on positioning of the transmembrane signaling helix of a chemoreceptor, *Mol. Micro. 61,* 1081-90.

58. Butler, S. L., and Falke, J. J. (1998) Cysteine and disulfide scanning reveals two amphiphilic helices in the linker region of the aspartate chemoreceptor, *Biochemistry 37*, 10746-56.

59. Aravind, L., and Ponting, C. P. (1999) The cytoplasmic helical linker domain of receptor histidine kinase and methyl-accepting proteins is common to many prokaryotic signalling proteins. *FEMS Microbiol. Lett. 176*, 111-6.

60. Williams, S. B., and Stewart, V. (1999) Functional similarities among two-component sensors and methyl-accepting chemotaxis proteins suggest a role for linker region amphipathic helices in transmembrane signal transduction, *Mol. Microbiol. 33*, 1093-1102.

61. Hulko, M., Berndt, F., Gruber, M., Linder, J. U., Truffault, V., Schultz, A., Martin, J., Schultz, J. E., Lupas, A. N., and Coles. M. (2006) The HAMP domain structure implies helix rotation in transmembrane signaling, *Cell 126,* 929-40.

62. Granseth, E., von Heijne, G., and Elofsson, A. (2005) A study of the membrane-water interface region of membrane proteins, *J. Mol. Biol. 346*, 377-85.

63. Braun, P., and von Heijne, G. (1999) The aromatic residues Trp and Phe have different effects on the positioning of a transmembrane helix in the microsomal membrane. *Biochemistry 38*, 9778-82.

64. de Planque, M. R., Bonev, B. B., Demmers, J. A., Greathouse, D. V., Koeppe, R. E., 2nd, Separovic, F., Watts, A., and Killian, J. A. (2003) Interfacial anchor properties of tryptophan residues in transmembrane peptides can dominate over hydrophobic matching effects in peptide-lipid interactions, *Biochemistry 42*, 5341-8.

65. Bass, R. B., Coleman, M. D., and Falke, J. J. (1999) Signaling domain of the aspartate receptor is a helical hairpin with a localized kinase docking surface: cysteine and disulfide scanning studies, *Biochemistry 38,* 9317-27.

66. Starrett, D. J., and Falke, J. J. (2005) Adaptation mechanism of the aspartate receptor: electrostatics of the adaptation subdomain play a key role in modulating kinase activity, *Biochemistry 44*, 1550-60.

67. Winston, S. E., Mehan, R., and Falke, J. J. (2005) Evidence that the adaptation region of the aspartate receptor is a dynamic four-helix bundle: cysteine and disulfide scanning studies. *Biochemistry 44*, 12655-66.

68. Ames, P., Studdert, C. A., Reiser, R. H., and Parkinson, J. S. (2002) Collaborative signaling by mixed chemoreceptor teams in *Escherichia coli*, *Proc. Natl. Acad. Sci. U.S.A. 99*, 7060-5.

69. Studdert, C. A., and Parkinson, J. S. (2004) Crosslinking snapshots of bacterial chemoreceptor squads, *Proc. Natl. Acad. Sci. U.S.A. 101*, 2117-22.

70. Studdert, C. A., and Parkinson, J. S. (2005) Insights into the organization and dynamics of bacterial chemoreceptor clusters through *in vivo* crosslinking studies, *Proc. Natl. Acad. Sci. U.S.A. 102*, 15623-8.

71. Ames, P., and Parkinson, J. S. (2006) Conformational suppression of inter-receptor signaling defects, *Proc. Natl. Acad. U.S.A. 103,* 9292-7.

72. Levit, M. N., and Stock, J. B. (2002) Receptor methylation controls the magnitude of stimulus-response coupling in bacterial chemotaxis, *J. Biol. Chem. 277,* 36760-5.

73. Lai, R.-Z., Manson, J. M., Bormans, A. F., Draheim, R. R., Nguyen, N. T., and Manson, M. D. (2005) Cooperative signaling among bacterial chemoreceptors, *Biochemistry 44*, 14298-307.

74. Maddock, J. R., and Shapiro, L. (1993) Polar localization of the chemoreceptor complex in the *Escherichia coli* cell, *Science 259,* 1717-23.

75. Shimizu, T. S., Le Novere, N., Levin, M. D., Beavil, A. J., Sutton, B. J., and Bray, D. (2000) Molecular model of a lattice of signalling proteins involved in bacterial chemotaxis, *Nat. Cell Biol. 2*, 792-6.

76. Sourjik, V. and Berg, H. C. (2000) Localization of components of the chemotaxis machinery of *Escherichia coli* using fluorescent protein fusions, *Mol. Micro. 37,* 740-51.

77. Kentner, D. and Sourjik, V. (2006) Spatial organization of the bacterial chemotaxis system, *Curr. Opin. Microbiol. 9,* 619-24.

78. White, S. H., and Wimley, W. C. (1999) Membrane protein folding and stability: physical principles, *Annu. Rev. Biophys. Biomol. Struct. 28,* 319-365.

79. de Planque, M. R., and Killian, J. A. (2003) Protein-lipid interactions studied with designed transmembrane peptides: role of hydrophobic matching and interfacial anchoring, *Mol. Mem. Biol. 20*, 271-84.

80. Nilsson, I., Saaf, A., Whitley, P., Gafvelin, G., Waller, C., and von Heijne, G. (1998) Proline-induced disruption of a transmembrane alpha-helix in its natural environment, *J. Mol. Biol 284*, 1165-75.

81. Killian, J. A., Salemink, I., de Planque, M. R., Lindblom, G., Koeppe, R. E., 2nd, and Greathouse, D. V. (1996) Induction of nonbilayer structures in diacylphosphatidylcholine model membranes by transmembrane alpha-helical peptides: importance of hydrophobic mismatch and proposed role of tryptophans, *Biochemistry 35*, 1037-45

82. Maeda, K., Imae, Y., Shioi, J. I., and Oosawa, F. (1976) Effect of temperature on motility and chemotaxis of *Escherichia coli, J. Bacteriol. 127*, 1039-46.

83. Yau, W. M., Wimley, W. C., Gawrisch, K., and White, S. H. (1998) The preference of tryptophan for membrane interfaces, *Biochemistry 37*, 14713-8.

84. Smith, R. A., and Parkinson, J. S. (1980) Overlapping genes at the *cheA* locus of *Escherichia coli*, *Proc. Natl. Acad. Sci. U.S.A. 77*, 5370-4.

85. Parkinson, J. S. (1978) Complementation analysis and deletion mapping of *Escherichia coli* mutants defective in chemotaxis, *J. Bacteriol. 135*, 45-53.

86. Weerasuriya, S., Schneider, B. M., and Manson, M. D. (1998) Chimeric chemoreceptors in *Escherichia coli*: signaling properties of Tar-Tap and Tap-Tar hybrids, *J. Bacteriol. 180*, 914-20.

87. Gardina, P., Conway, C., Kossman, M., and Manson, M. (1992) Aspartate and maltose-binding protein interact with adjacent sites in the Tar chemotactic signal transducer of *Escherichia coli*, *J. Bacteriol. 174*, 1528-36.

88. Guzman, L. M., Belin, D., Carson, M. J., and Beckwith, J. (1995) Tight regulation, modulation, and high-level expression by vectors containing the arabinose pBAD promoter, *J. Bacteriol. 177*, 4121-30.

89. Cantwell, B. J., Draheim, R. R., Weart, R. B., Nguyen, C., Stewart, R. C., and Manson, M. D. (2003) CheZ phosphatase localizes to chemoreceptor patches via CheA-short, *J. Bacteriol. 185*, 2354-61.

90. Southern, J. A., Young, D. F., Heaney, F., Baumgartner, W. K., and Randall, R. E. (1991) Identification of an epitope on the P and V proteins of simian virus 5 that distinguishes between two isolates with different biological characteristics, *J. Gen. Virol. 72 (Part 7)*, 1551-7.

91. Miller, J. H. (1972) in *Experiments in Molecular Genetics* p 433, Cold Spring Harbor Laboratory, Cold Spring Harbor, NY.

92. Berg, H. C., and Block, S. M. (1984) A miniature flow cell designed for rapid exchange of media under high-power microscope objectives, *J. Gen. Microbiol. 130*, 2915-20.

93. Gegner, J. A., Graham, D. R., Roth, A. F., and Dahlquist, F. W. (1992) Assembly of an MCP receptor, CheW, and kinase CheA complex in the bacterial chemotaxis signal transduction pathway, *Cell 70*, 975-82.

94. Hess, J. F., Bourret, R. B., and Simon, M. I. (1991) Phosphorylation assays for proteins of the two-component regulatory system controlling chemotaxis in *Escherichia coli*, *Methods Enzymol. 200*, 188-204.

95. Borkovich, K. A., and Simon, M. I. (1991) Coupling of receptor function to phosphate-transfer reactions in bacterial chemotaxis, *Methods Enzymol*. *200*, 205-14.

96. Bolivar, F., Rodriquez, R. L., Betlach, M. C., and Boyer, H. W. (1977) Construction and characterization of new cloning vehicles. II. A multipurpose cloning system, *Gene 2*, 95-113.

97. Zhu, Y., and Inouye, M. (2003) Analysis of the role of the EnvZ linker region in signal transduction using a chimeric Tar/EnvZ receptor protein, Tez1, *J. Biol. Chem. 278*, 22812-9.

98. Monne, M., Nilsson, I., Johansson, M., Elmhed, N., and von Heijne, G. (1998) Positively and negatively charged residues have different effects on the position in the membrane of a model transmembrane helix, *J. Mol. Biol. 284*, 1177-83.

99. Sharp, L. L., Zhou, J., and Blair, D. F. (1995) Tryptophan-scanning mutagenesis of MotB, an integral membrane protein essential for flagellar rotation in *Escherichia coli*, *Biochemistry 34*, 9166-71.

100. Sharp, L. L., Zhou, J., and Blair, D. F. (1995) Features of MotA proton channel structure revealed by tryptophan-scanning mutagenesis, *Proc. Natl. Acad. Sci. U.S.A. 92*, 7946-50.

101. Utsumi, R., Brissette, R. E., Rampersaud, A., Forst, S. A., Oosawa, K., and Inouye, M. (1989) Activation of bacterial porin gene expression by a chimeric signal transducer in response to aspartate, *Science 245*, 1246-9.

102. Baumgartner, J. W., Kim, C., Brissette, R. E., Inouye, M., Park, C., and Hazelbauer, G. L. (1994) Transmembrane signalling by a hybrid protein: communication from the domain of chemoreceptor Trg that recognizes sugar-binding proteins to the kinase/phosphatase domain of osmosensor EnvZ, *J. Bacteriol. 176*, 1157-63

103. Ward, S. M., Delgado, A., Gunsalus, R. P., and Manson, M. D. (2002) A NarX-Tar chimera mediates repellent chemotaxis to nitrate and nitrite, *Mol. Microbiol. 44*, 709-19.

104. Stock, J. B., and Surette, M. G. (1996). Chemotaxis, in *Escherichia col*i and *Salmonella* (Neidardt, F. C. et al., Eds.) pp 1103-1129, ASM Press, Washington, DC.

105. Francis, N. R., Wolanin, P. M., Stock, J. B., Derosier, D. J., and Thomas, D. R. (2004) Three-dimensional structure and organization of a receptor/signaling complex, *Proc. Natl. Acad. Sci. U.S.A. 101*, 17480-5.

106. Alon, U., Surette, M. G., Barkai, N., and Leibler, S. (1999) Robustness in bacterial chemotaxis, *Nature 397*, 168-71.

107. de Planque, M. R., Boots, J. W., Rijkers, D. T., Liskamp, R. M., Greathouse, D. V., and Killian, J. A. (2002) The effects of hydrophobic mismatch between phosphatidylcholine bilayers and transmembrane alpha-helical peptides depend on the nature of interfacially exposed aromatic and charged residues, *Biochemistry 41*, 8396-404.

108. Wolfe, A. J., and Berg, H. C. (1989) Migration of bacteria in semisolid agar, *Proc. Natl. Acad. Sci. U.S.A. 86*, 6973-7.

109. Ward, S. M., Bormans, A. F., and Manson, M. D. (2006) Mutationally altered signal output in the Nart (NarX-Tar) hybrid chemoreceptor, *J. Bacteriol. 188*, 3944-51.

110. Dwyer, M. A., Looger, L. L., and Hellinga, H. W. (2003) Computational design of a Zn^{2+} receptor that controls bacterial gene expression, *Proc. Natl. Acad. Sci. U.S.A. 100*, 11255-60.

111. Derr, P., Boder, E., and Goulian, M. (2006) Changing the specificity of a bacterial chemoreceptor, *J. Mol. Biol. 355*, 923-32.

112. Dwyer, M. A., and Hellinga, H. W. (2004) Periplasmic binding proteins: a versatile superfamily for protein engineering, *Curr. Opin. Struct. Biol. 14*, 495-504.

113. Ulrich, L. E., Koonin, E. V., and Zhulin, I. B. (2005) One-component systems dominate signal transduction in prokaryotes, *Trends Microbiol. 13*:52-6.

114. Beier, D., and Gross, R. (2006) Regulation of bacterial virulence by two component systems, *Curr. Opin. Microbio. 9*:143-52.

115. Calva, E., and Oropeza, R. (2006) Two-component signal transduction systems, environmental signals, and virulence, *Microb. Ecol. 51*:166-76.

116. Sonnhammer, E. L. L., von Heijne, G., and Krogh, A. (1998) A hidden Markov model for predicting transmembrane helices in protein sequences. In J. Glasgow, T. Littlejohn, F. Major, R. Lathrop, D. Sankoff, and C. Sensen, editors, Proceedings of the Sixth International Conference on Intelligent Systems for Molecular Biology, pages 175-182, Menlo Park, CA, AAAI Press.

117. Krogh, A. Larsson, B., von Heijne, G., and Sonnhammer, E. L. L. (2001) Predicting transmembrane protein topology with a hidden Markov model: Application to complete genomes, *J. Mol. Biol. 305*:567-80.

118. Williams, S. B., and Stewart, V. (1997) Nitrate- and nitrite-sensing protein NarX of *Escherichia coli* K-12: mutational analysis of the amino-terminal tail and first transmembrane segment, *J. Bacteriol. 179*:721-9.

119. Batchelor, E., and Goulian, M. (2003) Robustness and the cycle of phosphorylation and dephosphorylation in a two-component regulatory system, *Proc. Natl. Acad. Sci. U.S.A. 100*: 691-6.

120. Yamamoto, K., Hirao, K., Oshima, T., Aiba H., Utsumi, R., and Ishihama, I. (2005) Functional characterization *in vitro* of all two-component signal transduction systems from *Escherichia coli*, *J. Biol. Chem. 280*:1448-56.

121. Neiditch, M. B., Federle, M. J., Pompeani, A. J., Kelly, R. C., Swem, D. L., Jeffrey, P. D., Bassler, B. L., Hughson, F. M. (2006) Ligand-induced asymmetry in histidine sensor kinase complex regulates quorum sensing, *Cell 126,* 1095-108.

122. Hessa, T., Kim, H., Bihlmaier, K., Lundin, C., Boekel, J., Andersson, H., Nilsson, I., White, S. H., and von Heijne, G. (2005) Recognition of transmembrane helices by the endoplasmic reticulum translocon, *Nature 433,* 377-81.

VITA

Name: Roger Russell Draheim

Address: Stockholm Center for Biomembrane Research, Stockholm University, Department of Biochemistry and Biophysics, Svante Arrhenius väg 12, SE 106 91, Stockholm, Sweden

Email address: rogerdraheim@gmail.com

Education: Ph.D., Microbiology, Texas A&M University, 2007
B.S., Biochemistry and Microbiology, University of Maine, 1999
B.S., Cellular and Molecular Biology, University of Maine, 1999

Publications:

Draheim, R. R., Bormans, A. F., Lai, R.-Z., and Manson, M. D. (2006) Tuning a Bacterial Chemoreceptor with Protein-Membrane Interactions, *Biochemistry 45,* 14655-64.

Lai, R.-Z., Manson, J. M. B., Bormans, A. F., Draheim, R. R., Nguyen, N. T., and Manson, M. D. (2005) Cooperative Signaling among Bacterial Chemoreceptors, *Biochemistry 44,* 14298-307.

Draheim, R. R., Bormans, A. F., Lai, R.-Z., and Manson, M. D. (2005) Tryptophan Residues Flanking the Second Transmembrane Helix (TM2) Set the Signaling State of the Tar Chemoreceptor, *Biochemistry 44,* 1268-77.

Cantwell, B. J., Draheim, R. R, Weart, R. B, Nguyen, C., Stewart, R. C, Manson, M. D. (2003) CheZ Phosphatase Localizes to Chemoreceptor Patches via CheA-short, *J. Bacteriol. 185,* 2354-61.